Suppression of weak localization and enhancement of noise by tunneling in semiclassical chaotic transport

Robert S. Whitney
Institut Laue-Langevin, 6, rue Jules Horowitz, BP 156, 38042 Grenoble, France
(Received 5 December 2006; revised manuscript received 28 February 2007; published 5 June 2007)

We add simple tunneling effects and ray splitting into the recent trajectory-based semiclassical theory of quantum chaotic transport. We use this to derive the weak-localization correction to conductance and the shot noise for a quantum chaotic cavity (billiard) coupled to n leads via tunnel barriers. We derive results for arbitrary tunneling rates and arbitrary (positive) Ehrenfest time τ_E. For all Ehrenfest times, we show that the shot noise is enhanced by the tunneling, while the weak localization is *suppressed*. In the opaque barrier limit (small tunneling rates with large lead widths, such that the Drude conductance remains finite), the weak localization goes to zero linearly with the tunneling rate, while the Fano factor of the shot noise remains finite but becomes *independent* of the Ehrenfest time. The crossover from random matrix theory behavior ($\tau_E=0$) to classical behavior ($\tau_E=\infty$) goes exponentially with the ratio of the Ehrenfest time to the paired-path survival time. The paired-path survival time varies between the dwell time (in the transparent barrier limit) and half the dwell time (in the opaque barrier limit). Finally, our method enables us to see the physical origin of the suppression of weak localization; it is due to the fact that tunnel barriers "smear" the coherent-backscattering peak over reflection and transmission modes.

DOI: 10.1103/PhysRevB.75.235404 PACS number(s): 73.23.−b, 74.40.+k, 05.45.Mt, 05.45.Pq

I. INTRODUCTION

Semiclassical trajectory-based methods have long been applied to quantum chaos;[1,2] however, recent years have seen phenomenal progress in this field. The challenge of going beyond the Berry diagonal approximation[3] has finally been overcome.[4] Some works[4–10] have made progress toward a microscopic foundation for the well-established conjecture[11] that hyperbolic chaotic systems have properties described by random matrix theory (RMT). Other works[12–22] have explored the crossover from the RMT regime (negligible Ehrenfest time) to the classical limit (infinite Ehrenfest time). Most of the latter (and some of the former) works have dealt with mesoscopic effects in the quantum transport of electrons through open quantum dots with chaotic shape. They have analyzed the weak-localization correction to conductance and the resulting magnetoconductance,[5,7,12,14,16,18,19] the shot–noise (intrinsic quantum noise),[8,13,17,22] and conductance fluctuations.[20,21] However, to date, all such works on quantum transport have assumed perfect coupling to the leads. The objective of this work is to consider quantum transport through a chaotic system that is coupled to the leads via tunnel barriers (see Fig. 1). Such systems are experimentally realizable as large ballistic quantum dots.[23] We study two properties of quantum transport, which highlight different aspects of the wave nature of electrons. The first is the weak-localization correction to conductance; it is a contribution to conductance due to interference between electron waves. It is destroyed by a weak magnetic field, leading to a finite magnetoconductance. The second is the shot noise, an intrinsically quantum part of the fluctuations of a nonequilibrium electronic current; it is due to the fact that different parts of the electron wave can go to different places.

If one assumes that the chaotic system is well described by a random matrix from the appropriate random matrix ensemble, then it is known how to calculate transport through a chaotic system coupled to leads via tunnel barriers.[24,25] Under this assumption, it has been shown that a cavity with two identical leads (both with N modes and with barriers with tunneling probability ρ) has a Drude dimensionless conductance $g^{\mathrm{Drude}}=\rho N/2$, while the weak-localization correction goes like $g^{\mathrm{wl}}=-\rho/4$. Thus, the weak-localization correction goes to zero when we take $\rho\to 0$, even when one keeps the Drude conductance constant (by taking $N\to\infty$ such that ρN remains constant). The formal nature of the RMT derivations has made it hard to give a simple physical explanation of why this suppression of weak localization occurs. Indeed, the suppression seems counterintuitive, since we know that in a chaotic (ergodic and mixing) system the details of the system dynamics have little effect on the transport properties. Thus, one would expect that transport through a lead with such tunnel barriers should be equivalent to transport through a lead with $N'=\rho N$ modes without tunnel barriers. This argu-

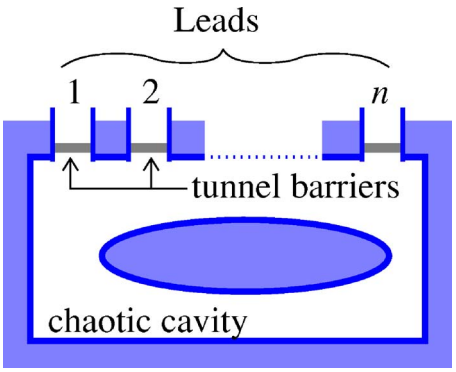

FIG. 1. (Color online) A chaotic cavity (billiard) with n leads. The mth lead has width W_m and is coupled to the cavity through a tunnel barrier with transmission probability ρ_m. We assume that all the tunnel barriers are very high and thin, so that this transmission probability is independent of the lead mode number.

 ©2007 The American Physical Society

ment predicts the correct Drude conductance; however, it would lead one to predict *incorrectly* that the weak-localization correction is $-1/4$, instead of $-\rho/4$. The vanishing of weak localization in the limit of strong tunneling is intriguing because it shows that there can be competition between two of the most fundamental aspects of quantum mechanics: tunneling and interference.

One problem with the random matrix assumption is that it tells us nothing about the crossover to the classical limit. The parameter which controls this crossover is the ratio of the Ehrenfest time to a dwell time. The Ehrenfest time (first introduced into chaotic quantum transport in Ref. 12) is given by the time it takes for a wave packet which is well localized in phase space to get stretched to a classical length scale. Since the wavelength $\lambda_F=\hbar/p_F$ is much smaller than the system size L, the stretching is well approximated by the flow of the classical dynamics. In a hyperbolic chaotic system, this stretching is exponential and happens at a rate given by the Lyapunov exponent λ. It is convenient to define the Ehrenfest time as twice the time for a minimal wave packet [spread by $(\lambda_F L)^{1/2}$ in position and $(\lambda_F L/\hbar)^{-1/2}$ in momentum] to stretch to a classical scale. Typically, in open chaotic systems, there are two classical scales, the system size L and the lead width W; there is an Ehrenfest time associated with each scale,[26,27]

$$\tau_E^{\mathrm{cl}} = \lambda^{-1} \ln[L/\lambda_F], \tag{1}$$

$$\tau_E^{\mathrm{op}} = \lambda^{-1} \ln[(L/\lambda_F)(W/L)^2]. \tag{2}$$

The first we call the *closed-cavity* Ehrenfest time, since it is the only Ehrenfest scale in a closed system, the second we call the *open-cavity* Ehrenfest time, because it is associated with the opening of the leads. However, we emphasize that both length scales (L and W) and, hence, both Ehrenfest times are relevant to open cavities.[17,18]

On times shorter than the Ehrenfest times, the dynamics of the system are not sufficiently mixing to give RMT results for transport quantities. In this paper, we address how tunneling affects transport when a significant proportion of the current is carried by paths shorter than the Ehrenfest times. To do this, we must include the ray splitting caused by such tunnel barriers into the semiclassical trajectory-based method. We then investigate the effect of tunneling on weak localization and intrinsic quantum noise (shot noise) in a system with finite Ehrenfest time. In addition to this, we find that the method enables us to clearly see the physical mechanism by which tunneling suppresses the weak-localization effects. The method presented here was used in Ref. 28 to investigate the effect of dephasing voltage probes on weak localization.

This paper is organized as follows. Section II contains qualitative explanations of the central results in this paper (particularly the suppression of weak localization and Ehrenfest independence of the shot noise in the opaque barrier limit). Section III discusses the dynamics of the classical paths which are relevant for the semiclassical calculations. Section IV sets up the formalism for including tunneling in the semiclassical trajectory-based method. Sections V and VI then present calculations of the weak-localization correction to conductance and the Fano factor of the shot noise, respectively.

II. QUALITATIVE DISCUSSION OF RESULTS

A. Suppression of weak localization by the smearing of the coherent-backscattering peak

As noted in Refs. 18 and 19 for a system without tunnel barriers, the coherent-backscattering approximately doubles the weight of all paths returning close and antiparallel to the same path at injection. The approximate doubling of the weight applies to all paths that return to a strip defined by (y,θ) across the lead, where

$$\theta - \theta_0 \simeq -p_F^{-1} m\lambda (y - y_0)\cos\theta_0 \tag{3}$$

for a path that was initially injected at (y_0,θ_0). This strip sits on the stable axis of the classical dynamics, with a width in the unstable direction of order $\hbar(p_F W)^{-1}$. The probability for the particle to go anywhere else is slightly reduced [by the weak-localization correction which is negative and (y,θ) independent]; this ensures that the probability for the particle to go somewhere remains 1 (preserving unitarity and conserving current). Since the enhancement due to coherent backscattering only occurs for reflection, we see that reflection is slightly enhanced and transmission (and hence conductance) is slightly reduced; this is the weak-localization correction to conductance.

However, once we introduce tunnel barriers, the situation becomes more complicated. There is still the enhancement of paths that return to close and antiparallel to themselves at injection; however, there is no longer a guarantee that this enhancement contributes to reflection. The enhanced paths can return to the injection lead but then be reflected off the tunnel barrier, remaining in the cavity [see Fig. 4(c)]. These enhanced paths will then bounce in the cavity until they eventually transmit through a barrier, either contributing to transmission [as shown in Fig. 4(c)] or reflection [as shown in Fig. 4(c) if we set $m=m_0$]. We use the term *successful coherent backscattering* to refer to the usual coherent-backscattering contribution, shown in Fig. 4(b), while using the term *failed coherent backscattering* for those contributions which behave in the manner shown in Figs. 4(c) and 4(d).

Thus, the failed coherent backscattering gives a positive contribution to both reflection and transmission, which will tend to offset the negative one coming from the usual weak-localization correction. This contribution will go like $(1-\rho)$ times the coherent-backscattering contribution in the absence of tunnel barriers. This contribution will be "smeared" over all leads with a weight for each lead equal to the probability of escaping through that lead. So, if the cavity has two identical leads, half of it will contribute to transmission and the other half to reflection. The successful coherent backscattering goes like ρ and only contributes to reflection.

As we take $\rho \to 0$, we see that the coherent backscattering becomes completely "failed" (the successful part goes to zero). So, the whole backscattering peak is smeared over all leads in exactly the same way as the conventional weak-

localization correction. Both have a weight for any given lead equal to the probability for the particle to escape through that lead. However, the two have opposite signs (which they must to preserve unitarity) and thereby cancel. Hence, the total weak-localization correction [sum of the usual weak-localization correction, Fig. 4(a), and the failed coherent backscattering, Figs. 4(c) and 4(d)] vanishes when we take $\rho \to 0$ (even if we keep ρN finite, so the Drude conductance remains finite).

B. RMT to classical crossover given by ratio of Ehrenfest time to paired-path survival time

In all calculations in this paper, we find that the crossover from RMT behavior (zero Ehrenfest time) to classical behavior (infinite Ehrenfest time) is governed by the ratio of the Ehrenfest time to the *paired-path* survival time, and not the *single-path* survival time (the dwell time). The paired-path survival time, defined in Eq. (13), is the time during which a pair of initially identical classical paths both remain inside the cavity. Under the classical dynamics of a closed cavity, a pair of initially identical paths remains paired (identical) forever. However, the presence of the leads means that all paths remain for a finite time in the cavity; we call this the dwell time or single-path survival time τ_{D1}. Further, if there are tunnel barriers on the leads, then the paired-path survival time τ_{D2} is given by the time for one or both of two (initially identical) paths to escape. We show that this time varies between τ_{D1} for transparent barriers to $\frac{1}{2}\tau_{D1}$ for opaque barriers.

The reason why τ_{D2} is the relevant time scale for the suppression of the crossover is as follows. All paths which contribute to the RMT limit must involve an intersection at an angle of order $(\lambda_F/L)^{1/2}$, and the paths must survive in the cavity until they spread to a distance apart of order of the width of the lead on both sides of the intersection. Within $\frac{1}{2}\tau_E^{\mathrm{op}}$ on either side of the intersection, the paths are correlated, and so their joint survival probability decays at the rate of τ_{D2}^{-1}. The shot-noise contributions is divided into those in which the paired paths survive for a time less than τ_E^{op} and those which survive a time greater than τ_E^{op}. Thus, we see that these contributions go like $(1-\exp[-\tau_E^{\mathrm{op}}/\tau_{D2}])$, and $\exp[-\tau_E^{\mathrm{op}}/\tau_{D2}]$, respectively.

All weak-localization contributions require that the path segments diverge to a distance of order of the system size on one side of the intersection (so that a closed loop can form) and to a distance of order of the lead width on the other side (when the "legs" can escape). Thus, the path segments must survive until a time τ_E^{cl} on the loop side of the intersection and τ_E^{op} on the leg side. However, within $\tau_E^{\mathrm{op}}/2$ on both sides of the intersection, the paths have the paired-path survival probability (because they are closer than the lead width), while elsewhere each path segment individually has the single-path escape probability. Thus, we see that the exponential suppression of weak localization for finite Ehrenfest time goes like the survival probability for such paths of length $\tau_E^{\mathrm{op}}+\tau_E^{\mathrm{cl}}$ which is

$$\exp[-\tau_E^{\mathrm{op}}/\tau_{D2}-(\tau_E^{\mathrm{cl}}-\tau_E^{\mathrm{op}})/\tau_{D1}]. \tag{4}$$

The first term in the exponent is the Ehrenfest time dependence, and the second term is a classical correction, since $(\tau_E^{\mathrm{cl}}-\tau_E^{\mathrm{op}})$ is independent of the particle wavelength. In the transparent barrier limit (where $\tau_{D2}=\tau_{D1}$), the suppression goes like $\exp[-\tau_E^{\mathrm{cl}}/\tau_{D1}]$ as found in Ref. 18, while in the opaque barrier limit, we find $\tau_{D2}=\tau_{D1}/2$ so the suppression goes like $\exp[-(\tau_E^{\mathrm{cl}}+\tau_E^{\mathrm{op}})/\tau_{D1}]$.

In general, the survival probability of such intersecting paths of total length $t>2\tau_E^{\mathrm{op}}$ is

$$\exp[-(t-2\tau_E^{\mathrm{op}})/\tau_{D1}-\tau_E^{\mathrm{op}}/\tau_{D2}], \tag{5}$$

since the paths are paired during a time τ_E^{op} and unpaired at all other times (when unpaired, each segment decays at a rate of τ_{D1}^{-1}). In the transparent barrier limit, this is $\exp[-(t-\tau_E^{\mathrm{op}})/\tau_{D1}]$, while in the opaque barrier limit, it is simply $\exp[-t/\tau_{D1}]$.

C. Ehrenfest time independence of shot noise in the opaque barrier limit

In the limit of opaque barriers (small tunneling rate), we find that the shot noise is independent of the Ehrenfest time up to first order in ρ, see Eq. (75). Thus, for any small ρ, the magnitude of the difference between the noise in the RMT limit ($\tau_E^{\mathrm{op}}=0$) and the classical limit ($\tau_E^{\mathrm{op}}=\infty$) goes like ρ^2 and thus may be beyond experimental resolution. This is despite the fact that the contributions in the RMT limit are very different from those in the classical limit. Closer inspection shows that those contributions which survive in the opaque limit [Figs. 6(e)–6(i) and 7(b)–7(g)] do have one thing in common; none of them have correlations between the paths when entering or exiting the cavity. Thus, it appears that it is irrelevant whether correlated paths have enough time to become uncorrelated inside the cavity (as they do when $\tau_E^{\mathrm{op}} \ll \tau_{D2}$, but not when $\tau_E^{\mathrm{op}} \gg \tau_{D2}$) because the tunnel barriers destroy all correlations between paths (the probability that both paths exit when they hit the tunnel barrier is zero in this limit). It is intriguing that the shot noise is so insensitive to the manner in which correlations between paths are destroyed (either via classical dynamics or via tunneling).

We note that for a symmetric two-lead system in the opaque limit ($N_1=N_2$ and $\rho_1=\rho_2 \ll 1$), the shot noise is half that for Poissonian noise (Fano factor $F=1/2$). Thus, even though the transmission probability is small, and so transmission is rare, the transmission is a sub-Poissonian process. The fermionic nature of the electrons induces correlations even in this limit. The result that $F=1/2$ is the same as one would get for two leads coupled by a single tunnel barrier with transmission probability equal to 1/2 (with no chaotic system present at all).

III. CLASSICAL DYNAMICS IN A SYSTEM WITH TUNNEL BARRIERS ON THE LEADS

In this paper, we consider a quantum system whose classical limit (wavelength $\lambda_F \to 0$) has a nonzero tunneling probability at tunnel barriers (we assume the width of the barriers scales with λ_F). Thus, it is natural to include tunneling at the level of the classical dynamics. Here, we introduce tunneling into the classical dynamics phenomenologically; we will then see in Sec. IV that it is the classical limit of the

quantum problem we wish to solve. We assume that each time a classical path hits a barrier, there is a probability of ρ that the path goes through the barrier (as if the barrier were absent) and a probability of $(1-\rho)$ that the particle is specularly reflected (as if the barrier were impenetrable).

The probabilistic nature of this tunneling makes the classical dynamics *stochastic*. The classical paths, which are the solutions of these stochastic dynamics, have properties not present in deterministic dynamics, such as bifurcations (ray splitting) at the tunnel barriers (one part transmitting and the other reflecting). To simplify the considerations in this paper, we consider tunnel barriers that have a tunneling probability which is independent of the angle θ at which a classical path hits the barrier. This assumption is justified for tunnel barriers in the limit of large barrier height and small barrier thickness (see Appendix A). This is equivalent to saying that we consider the tunnel barriers to have the same tunnel probability for all lead modes.

Let us now consider the dynamics of a classical particle in such a system. We define $\tilde{P}(\mathbf{Y},\mathbf{Y}_0;t)$ such that the classical probability for a particle to go from an initial position and momentum angle of $\mathbf{Y}_0 \equiv (y_0,\theta_0)$ in the phase space of lead m_0 (a point on the cross section of the lead just to the lead side of the tunnel barrier) to within $(\delta y,\delta\theta)$ of $\mathbf{Y}=(y,\theta)$ on the cross section of lead m (again just to the lead side of the tunnel barrier) in a time within δt of t is

$$\tilde{P}(\mathbf{Y},\mathbf{Y}_0;t)\delta y\,\delta\theta\delta t. \tag{6}$$

In a system *without* tunnel barriers, the classical dynamics is deterministic, and $\tilde{P}(\mathbf{Y},\mathbf{Y}_0;t)$ has a Dirac δ function with unit weight on classical paths. However, in a system *with* tunnel barriers, the classical dynamics is stochastic, with each barrier acting as a *ray splitter*. A classical path which hits a barrier is split into 2 (one which passes through the barrier and one which reflects). Thus, $\tilde{P}(\mathbf{Y},\mathbf{Y}_0;t)$ has a δ function on each classical path which exists (counting all possible ray splittings); however, the weight of the Dirac δ function is the product of the tunneling/reflection probabilities that that path has acquired each time it has hit a tunnel-barrier. Thus the integral of $\tilde{P}(\mathbf{Y},\mathbf{Y}_0;t)$ over all positions/momenta at escape, $\mathbf{Y}$, gives a sum over all paths starting from $\mathbf{Y}_0$ in which each term is weighted by these tunneling and/or reflection probabilities; hence,

$$\int_0^\infty dt \int d\mathbf{Y}\tilde{P}(\mathbf{Y},\mathbf{Y}_0;t)[\cdots]_{\mathbf{Y}_0} = \sum_{\gamma\in\{\mathbf{Y}_0\}} \rho_m\rho_{m_0}\prod_{m'}[1-\rho_{m'}]^{n_\gamma(m')}[\cdots]_\gamma, \tag{7}$$

where $d\mathbf{Y}=dyd\theta$, with y integrated over the cross section on each lead and θ integrated from $-\pi/2$ to $\pi/2$. The sum is over all possible path starting at $\mathbf{Y}_0\equiv(y_0,p_{y_0})$. Lead m is defined as the lead the path finally escapes into, and $n_\gamma(m')$ is the number of times that the path γ reflects off the tunnel barrier on lead m' before escaping. We assume that any quantities in $[\cdots]_\gamma$ are independent of $\rho_{m'}$; in other words, they are the same as for the path which would exist if the tunnel barriers were impenetrable for each reflection and absent for each tunneling of path γ.

In semiclassics, one is typically summing over all paths γ from y_0 to y with energy E rather than all paths starting at $\mathbf{Y}_0$. Using Eq. (7), we see that this sum can be written in terms of $\tilde{P}(\mathbf{Y},\mathbf{Y}_0;t)$ as

$$\sum_{\gamma\in\{y_0\to y;E\}} \rho_m\rho_{m_0}\prod_{m'}[1-\rho_{m'}]^{n_\gamma(m')}[\cdots]_\gamma = \int_0^\infty dt\int_{-\pi/2}^{\pi/2} d\theta_0 d\theta\left(\frac{dy}{d\theta_0}\right)\tilde{P}(\mathbf{Y},\mathbf{Y}_0;t)[\cdots]_{\mathbf{Y}_0}, \tag{8}$$

where the factor of $(dy/d\theta_0)$ comes from the change of integration variable from y to θ_0.

Ensemble or energy average of classical probabilities

If we average, $\langle\cdots\rangle$, over energy or an ensemble of similar chaotic systems, the average of $\tilde{P}(\mathbf{Y},\mathbf{Y}_0;t)$ will be a smooth function. If the system is mixing (when the leads are absent) and we perform sufficient averaging, we can assume that the probability to go to any place in the cavity phase space is uniform. From this, it immediately follows that the probability to go from a point in lead m_0 to anywhere in lead m (for $m\neq m_0$) is

$$\int_0^\infty dt\int_m d\mathbf{Y}\langle\tilde{P}(\mathbf{Y},\mathbf{Y}_0;t)\rangle = \rho_{m_0}\frac{\rho_m W_m}{\sum_{m'}\rho_{m'}W_{m'}} = \frac{\rho_{m_0}\rho_m N_m}{\sum_{m'}\rho_{m'}N_{m'}}, \tag{9}$$

where $\mathbf{Y}$ is integrated over the cross section of lead m. To see this, we simply note that the probability to enter the cavity from lead m_0 is ρ_{m_0}, and the probability to escape the cavity is 1. Thus, the probability to escape into lead m is the ratio of $\rho_m W_m$ to the sum of $\rho_{m'}W_{m'}$ over all leads. Note that in doing this, we ignore all unsuccessful attempts to escape; thus, the particle may have hit tunnel barriers on the leads many times, but each time is reflected. The result in Eq. (9) can also be derived by noting that the probability of hitting the tunnel barrier on lead m_i is $W_{m_i}/(\tau_0 L)$, where τ_0 is the time of flight across the cavity, and then explicitly summing all reflections off the barriers. However, we feel the above logic of ignoring all unsuccessful escape attempts gives the results in a direct and simpler manner; thus, we use it throughout this paper.

Following the same logic that leads to Eq. (9), we see that the survival probability of a single classical path which is inside the cavity is given by the following master equation:

$$\dot{P}_1(t) = -\tau_{D1}^{-1}P_1(t), \tag{10}$$

where we define the single-path dwell time as

$$\tau_{D1}^{-1} = (\tau_0 L)^{-1}\sum_{m=1}^{n}\rho_m W_m. \tag{11}$$

Thus, the probability to tunnel into the cavity from lead m_0 and then escape into lead m at position $\mathbf{Y}=(y,\theta)$ on the

phase-space cross section just to the lead side of the tunnel barrier is

$$\langle \tilde{P}(\mathbf{Y},\mathbf{Y}_0;t)\rangle = \frac{\rho_{m_0}\rho_m \cos\theta}{2\left(\sum_{m'}\rho_{m'}W_{m'}\right)\tau_{D1}} \exp[-t/\tau_{D1}]. \quad (12)$$

Now, we turn to the evolution of a pair of almost identical paths. A quick glance at the figures in this paper show that such pairs of paths (vertically cross-hatched regions in Figs. 3–9) are crucial to the quantities we calculate. This situation is different from the evolution of two very different paths, because here the two paths explore the same regions of the cavity's phase space. Thus, if one path hits a tunnel barrier, then so will the other one. This leads to the definition of "almost identical;" the paths must be a perpendicular distance apart that is less than the lead width for a significant period of time (at least a few bounces), i.e., their difference in momenta is less than $p_F \times W/L$. (In principle, two paths with very different momenta will be almost identical very close to the points where they cross; however, we ignore this as it will not significantly affect our calculations.) Then, when the pair of paths hits a tunnel barrier, the probability to survive (probability for both paths to remain in the cavity) is $(1-\rho_m)^2$; this means the probability to *not* survive is $\rho_m(2-\rho_m)$. Thus, the survival probability of paired paths is given by the master equation

$$\dot{P}_2(t) = -\tau_{D2}^{-1}P_2(t), \quad (13)$$

where we define the paired-path survival time as

$$\tau_{D2}^{-1} = (\tau_0 L)^{-1}\sum_{m=1}^{n}\rho_m(2-\rho_m)W_m. \quad (14)$$

Note that this is the probability that both paths survive. Since $0 \leqslant \rho_m \leqslant 1$, we see that $1 \leqslant \tau_{D1}/\tau_{D2} \leqslant 2$, with $\tau_{D2}=\tau_{D1}$ when all tunnel barriers are transparent ($\rho_m=1$ for all m) and $\tau_{D2}=\tau_{D1}/2$ in the limit of opaque barriers ($\rho_m \to 0$ for all m). Unfortunately, we cannot write down an equation for the evolution of pairs of paths which is as simple as Eq. (12), because even under averaging, the position (momentum) of the second path in the pair is *deterministically* given by its initial position (momentum) relative to the first path. Assuming the system has locally uniform hyperbolic dynamics (on length scales up to $W \ll L$), then the dynamics of the second path in coordinates perpendicular to the first is

$$\frac{d}{dt}\begin{pmatrix} r_\perp/L \\ p_\perp/p_F \end{pmatrix} = \mathcal{M}\begin{pmatrix} r_\perp/L \\ p_\perp/p_F \end{pmatrix}, \quad (15)$$

where $\mathcal{M}$ is a 2×2 matrix. For Hamiltonian dynamics, $\mathcal{M}$ has eigenvalues $\pm\lambda$ where λ is the Lyapunov exponent, and so the dynamics is area preserving. We will assume for simplicity that the eigenvector of $\mathcal{M}$ with eigenvalue $\pm\lambda$ is along the axis defined by $p_\perp = \pm m\lambda r_\perp$. We will use this to calculate the relative position of the second path in a pair when it is needed in the calculations below.

IV. TRAJECTORY-BASED SEMICLASSICS WITH TUNNEL BARRIERS

The semiclassical derivation of the Drude conductance has become standard[2,29] (here, we will broadly follow Ref. 18). However, we wish to introduce tunneling into this derivation; this presents a difficulty since tunneling cannot be described in conventional semiclassics. To deal with this, we follow a well-established procedure for dealing with a semiclassical system (wavelength much less than other length scales) in which there are isolated regions where semiclassics fails, see, for example, Ref. 30. We treat the regions where semiclassics fails in an exact manner (or using an appropriate approximation scheme) and then couple the propagators in those regions with the semiclassical ones in the regions where semiclassics works well.[31]

A. Energy Green's function and scattering matrix elements

Before addressing the construction of an energy Green's function which includes the tunneling, let us consider the case of a *ray* inside the cavity hitting the tunnel barrier on one of the leads. A ray is a plane wave multiplied by an envelope function in the direction perpendicular to its motion, which is much wider than λ_F but much narrower than the classical scales W and L. In this case, we can treat the scattering of the ray in the same manner as a plane wave hitting the tunnel-barrier on a lead of infinite width. The equations for motion parallel and perpendicular to the barrier can be solved separately. The evolution perpendicular to the barrier is given by the solution of a textbook one-dimensional tunneling problem (see Appendix A), while the evolution parallel to the barrier is unchanged by the presence of the barrier. The solution of the one-dimensional tunneling problem tells us that for any given ray arriving at the tunnel barrier, there will be two rays leaving the tunnel barrier. One ray is that transmitted through the barrier, has complex amplitude t, and has the same momentum as the incoming ray. The other ray is that reflected off the barrier, has complex amplitude r, and has its momentum perpendicular to the barrier reversed (specular reflection). Thus, each ray will be split into two each time it encounters a tunnel barrier. Of course, the amplitude of the two new rays are such that $|r|^2+|t|^2=1$. To fit with the classical model in Sec. III, we define $\rho=|t|^2$.

For a very narrow barrier (which is the only case we consider in this paper), these two rays are identical to the rays one would have if the barrier was both absent (transmitted ray) and impenetrable (reflected ray), except that here the amplitudes of the rays are multiplied by the complex amplitudes t and r, respectively. For such narrow tunnel barriers, the amplitudes t and r are independent of the angle θ of the incoming ray.

Now, we must do the same for the energy Green's function for propagating from r_0 in the L lead to r in the R lead. We do this in a manner similar to Ref. 30. We first note that at large distances, $|\mathbf{r}-\mathbf{r}_0| \gg \lambda_F$, a semiclassical Green's function $G(\mathbf{r},\mathbf{r}_0;E)$ is well approximated by a plane wave in the vicinity of any given classical path. Further, for $\mathbf{r} \neq \mathbf{r}_0$, the differential equations for the Green's function and a wave

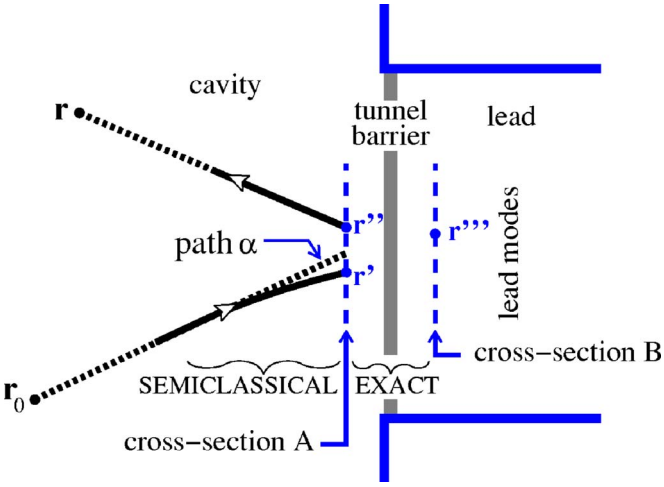

FIG. 2. (Color online) Schematic of the calculation of Green's functions in the vicinity of a tunnel barrier. The evolution from $\mathbf{r}' \to \mathbf{r}''$ and $\mathbf{r}' \to \mathbf{r}'''$ is treated exactly, while semiclassics is used for the evolution from $\mathbf{r}_0 \to \mathbf{r}'$ and $\mathbf{r}'' \to \mathbf{r}$. We calculate the contribution for the part of the incoming Green's function due to paths in the vicinity of the classical path α by matching the semiclassical and exact solutions of the Green's function equation on cross section A, which is just to the left of the tunnel barrier. Just to the right of the tunnel barrier, on cross section B, we couple to the lead modes.

function are the same (the Schrödinger equation). Thus, we treat the semiclassical Green's function in the vicinity of a given path which touches the tunnel barrier (path α) as a plane wave or ray. We use this as the ingoing boundary condition on cross section A (see Fig. 2) for the tunneling-reflection problem. The tunneling-reflection problem is solved using the standard method for wave functions (see Appendix A). The transmitted part gains a complex prefactor t and then couples to the lead modes (as in the case without tunnel barriers, we assume that the leads are wide enough that they accept all momentum states). The reflected part gains a complex amplitude r and is a plane wave with its momentum perpendicular to the barrier reversed compared with the incoming plane wave. Treating this outgoing plane wave, at cross section A, as a boundary condition on the semiclassical evolution, we see that it couples to exactly the same paths as if the barrier were impenetrable. Hence, every tunnel barrier couples each incoming path to two outgoing paths (one as if the barrier were absent and one as if the barrier were impenetrable). If the weight on the incoming path is B_α, then the weight on the two outgoing paths will be tB_α and rB_α for transmission and reflection at the barrier, respectively.

Hence, when we write the semiclassical Green's function inside the cavity in the usual way, it is a sum over classical paths inside the cavity which can either transmit or reflect at each barrier. The properties of the classical path (action S_γ, Maslov index μ_γ, and classical stability) are the same as for the classical path that would exist if the barrier were absent for each transmission and impenetrable for each reflection. The full energy Green's function, including the tunnel barriers, then takes the form $\Sigma_\gamma B_\gamma \exp[\mathrm{i}S_\gamma/\hbar + \mathrm{i}\mu_\gamma/2]$, where B_γ is the square root of the stability of the path multiplied by a complex factor of $t_{m'}$ and $r_{m'}$ for each transmission and reflection at barrier m'. Using Ref. 29 to go from this Green's function to the formula for $\mathrm{S}_{mm_0;ji}$, the scattering matrix element to go from mode i on lead m_0 to mode j on lead m, we get

$$\mathrm{S}_{mm_0;ji} = -(2\pi\mathrm{i}\hbar)^{-1/2} \int_{\mathrm{L}} dy_0 \int_{\mathrm{R}} dy \sum_\gamma A_\gamma \langle j|y\rangle\langle y_0|i\rangle \exp[\mathrm{i}S_\gamma/\hbar + \mathrm{i}\pi\mu_\gamma/2], \tag{16}$$

where $|i\rangle$ is the transverse wave function of the ith mode on lead m'. The sum is over all paths γ (with classical action S_γ and Maslov index μ_γ), which start at y_0 on the cross section of the injection (m_0) lead, tunnel into the cavity, and bounce many times (including reflecting off the tunnel barriers on the leads) before tunneling into lead m at point y on its cross section. The complex amplitude A_γ is

$$A_\gamma = \left(\frac{dp_{y_0}}{dy}\right)_\gamma^{1/2} t_m t_{m_0} \prod_{m'} [r_{m'}]^{n_\gamma(m')}, \tag{17}$$

where path γ starts from $\mathbf{Y}_0 = (y_0, p_{y_0})$ on lead m_0 and tunnels into the cavity, it then bounces inside the cavity, and finally it transmits through barrier m to end at $\mathbf{Y} = (y, p_y)$ in lead m. We define $n_\gamma(m')$ as the number of times that the path γ reflects off the tunnel barrier on lead m' before escaping. The differential $(dp_{y_0}/dy)_\gamma$ is the rate of change of initial momentum p_{y_0} with final position y for an *unchanged set* of transmissions and reflections at the barriers.

B. Landauer-Büttiker formula and the Drude conductance

Inserting Eq. (16) into the Landauer-Büttiker formula for the conductance

$$g_{mm_0} = \mathrm{Tr}[\mathrm{S}^\dagger_{mm_0} \mathrm{S}_{mm_0}], \tag{18}$$

one gets a double sum over paths $\gamma 1$ and $\gamma 2$ and over lead modes $|n\rangle$ and $|m\rangle$. We make a semiclassical approximation (see Appendix B) that $\Sigma_n \langle y'|n\rangle\langle n|y\rangle \simeq \delta(y'-y)$. The conductance is then given by a double sum over paths which both go from y_0 on lead m_0 to y on lead m as follows:

$$g_{mm_0} = (2\pi\hbar)^{-1} \int_{\mathrm{L}} dy_0 \int_{\mathrm{R}} dy \sum_{\gamma 1,\gamma 2} A_{\gamma 1} A^*_{\gamma 2} e^{\mathrm{i}\delta S/\hbar}. \tag{19}$$

where the action difference $\delta S = S_{\gamma 1} - S_{\gamma 2}$.

We averaged the conductance over the energy or the cavity shape. For most $\{\gamma 1, \gamma 2\}$, the phase of a given contribution, $\delta S/\hbar$, will oscillate wildly with these variations, so the contribution averages to zero. The only contributions that will survive are those in which $\gamma 1$ and $\gamma 2$ are correlated in such a manner that δS remains fixed when we vary the energy or the cavity shape. The most obvious such contributions[3] are diagonal ones ($\gamma 1 = \gamma 2$), and we now show that they give the Drude conductance.

For these diagonal contributions, we note that $(dp_{y_0}/dy)_\gamma = p_F \cos\theta_0 (d\theta_0/dy)_\gamma$ and then use Eq. (8) with $\rho_{m'} = |t_{m'}|^2 = 1 - |r_{m'}|^2$ to write the sum over all paths γ from y_0 to y as

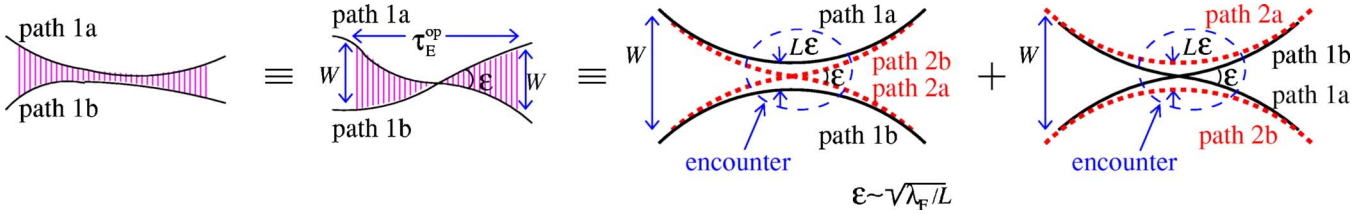

FIG. 3. (Color online) In all figures of contributions in this paper, we mark the regions where paths are correlated with vertical cross hatching. The encounter is at the center of those regions. The diagonal approximation is good everywhere except at the encounter; thus, for simplicity, we show only two of the four paths (or path segments) in all other figures in this paper. Here, we show what the cross-hatched regions in the other figures mean in terms of all four paths that enter them. In the cross-hatched region the two paths marked by solid lines are paired with each other. This region is macroscopic in size, the length of the region in time is $\tau_E^{\rm op}$ (which we assume to be of similar magnitude to the classical time scales such as τ_{D1} and τ_{D2}), and the distance between the paths at either end of this region is of order of the lead width. In contrast, the encounter (where both paths marked by dashed lines swap from one path marked by a solid line to the other) is microscopic in size, the distance between the noncrossing paths is typically $(\lambda_F L)^{1/2}$ which goes to zero in the classical limit, and the time which the encounter takes is a few times the inverse of the Lyapunov exponent.

$$\sum_\gamma |A_\gamma|^2[\cdots]_\gamma = \int_0^\infty dt \int_{-\pi/2}^{\pi/2} d\theta_0 d\theta P(\mathbf{Y},\mathbf{Y}_0;t)[\cdots]_{\mathbf{Y}_0}, \tag{20}$$

where for compactness we define $P(\mathbf{Y},\mathbf{Y}_0;t)=p_F\cos\theta_0 \times \tilde{P}(\mathbf{Y},\mathbf{Y}_0;t)$, with $p_F\cos\theta_0$ being the initial momentum along the injection lead. Using Eq. (9), we see that

$$\langle P(\mathbf{Y},\mathbf{Y}_0;t)\rangle = \frac{\rho_{m_0}\rho_m p_F \cos\theta_0 \cos\theta}{2\left(\sum_{m'}\rho_{m'}W_{m'}\right)\tau_{D1}} \exp[-t/\tau_{D1}]. \tag{21}$$

Using Eqs. (20) and (21), one finds the Drude conductance

$$g^D_{mm_0} = (1-\rho_{m_0})N_{m_0}\delta_{mm_0} + \frac{\rho_{m_0}N_{m_0}\rho_m N_m}{\sum_{m'}\rho_{m'}N_{m'}}. \tag{22}$$

The first term above is for reflection (δ_{mm_0} is a Kronecker delta function); it represents contributions which are reflected off the barrier on the injection lead without ever entering the cavity.

V. WEAK-LOCALIZATION CORRECTION TO CONDUCTANCE FOR A CHAOTIC SYSTEM WITH TUNNEL BARRIERS

We identify four contributions to the weak-localization correction to the conductance of a system coupled to leads via tunnel barriers. They are shown in Fig. 4.

A. Usual weak localization

Here, we consider the usual contribution to weak localization (wl0), the first contribution shown in Fig. 4. We call it the *usual* contribution because it is the only weak-localization contribution to transmission ($m\neq m_0$) when the tunnel barriers are absent ($\rho_m=1$ for all m). In this contribution, the paths are paired almost everywhere except in the vicinity of an encounter.[5] At an encounter, shown in detail in Fig. 3, one of the paths intersects itself, while the other one avoids the crossing. Reference 4 showed that every self-intersecting path with a small crossing angle ϵ has a partner which avoids the crossing. As a result, the two paths travel along the loop that they form in opposite directions. However, the two paths are always close enough to each other that they have the same stability; hence, $\Sigma_{\gamma 1,\gamma 2}A_{\gamma 1}A^*_{\gamma 2} \to \Sigma_{\gamma 1}|A_{\gamma 1}|^2$. To evaluate the usual weak-localization contribution (wl0), we perform a calculation similar to Ref. 18; this broadly follows Refs. 5 and 14 while adding the crucial fact that close to the encounter (the cross-hatched region in Fig. 4), the paths have a different survival probability from elsewhere. For a system with the tunnel barriers, the survival probability is given by Eq. (13) inside the cross-hatched region and given by Eq. (10) elsewhere.

As in Ref. 18, we only consider those contributions where the paths are uncorrelated when they hit the lead (by which we mean a collision with a lead where at least one pair of paths tunnels out of the system). Those contributions in which the paths are correlated when one of them tunnels out of the system are included in the coherent-backscattering contributions. Uncorrelated escape requires a minimal time $T_W(\epsilon)/2$ between encounter and escape, where[32]

$$T_W(\epsilon) = \lambda^{-1}\ln[\epsilon^{-2}(W/L)^2] \tag{23}$$

for a small crossing angle ϵ (see Fig. 3) in a system with Lyapunov exponent λ, system size L, and lead width W. This is because this is the time for the perpendicular distance between the paths to become larger than the width of the leads. Only then will the two paths escape in an uncorrelated manner, typically at completely different times, with completely different momenta (and possibly through different leads).

To calculate the contribution of the sum over all paths of the form sketched in Fig. 4, we note that the action difference δS is[4,5]

$$\delta S_{\rm wl} = E_F\epsilon^2/\lambda. \tag{24}$$

This assumes that the dynamics in the vicinity of the encounter is time-reversal symmetric; this is the case for any applied magnetic field which is weak enough not to affect the classical dynamics. We write the probability to go from $\mathbf{Y}_0$ to $\mathbf{Y}$ in time t in terms of the product of two probabilities. The

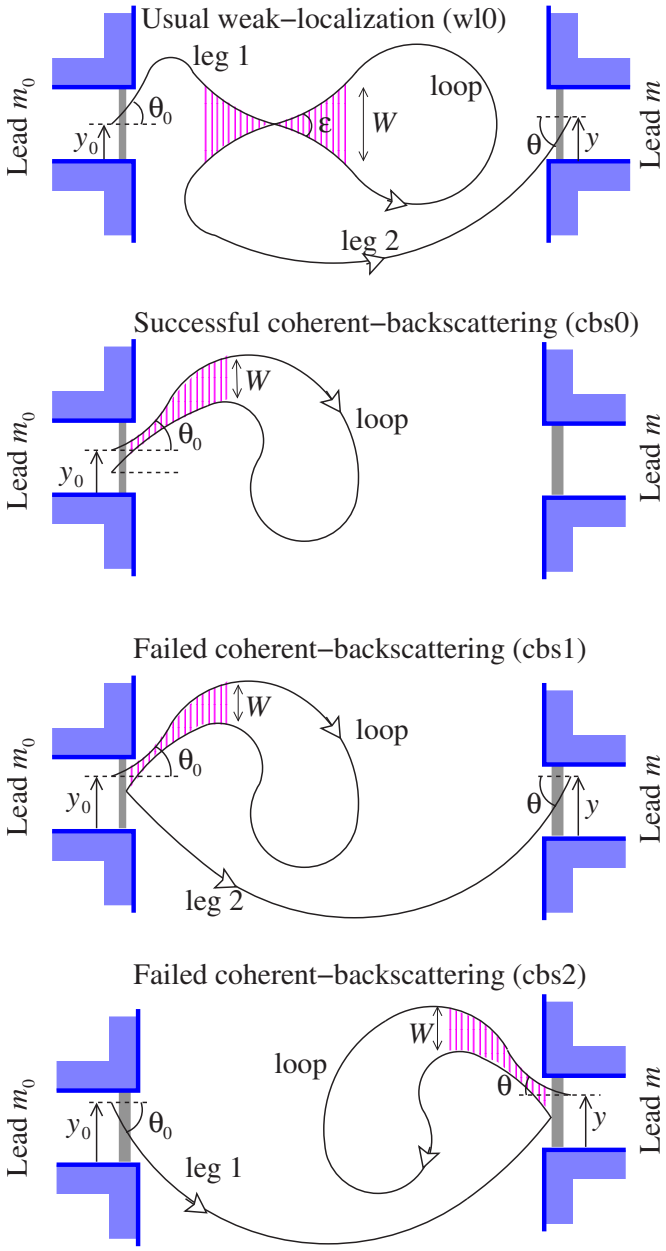

FIG. 4. (Color online) Weak-localization contributions to conductance (contributions to conductance of order N^0) when there are tunnel barriers on the leads. All contributions except the second are for any m_0 and m, while the second (cbs0) is only for $m=m_0$. The vertical cross hatching indicates the regions in which the paths are correlated with each other, so their survival probability is given by Eq. (13) and not by Eq. (10). The encounter occurs at the center of the correlated region, as shown in Fig. 3. Details of the correlated regions for successful and failed coherent backscatterings are shown in Fig. 5.

first is probability to go from $\mathbf{Y}_0$ to a point on the energy surface inside the cavity $\mathbf{R}_1=(\mathbf{r}_1,\phi_1)$ (where ϕ_1 defines the direction of the momentum) in time t_1. The second is the probability to go from $\mathbf{R}_1$ to $\mathbf{Y}$ in time $t-t_1$. When one integrates this product over $\mathbf{R}_1$ on the energy surface $\mathcal{C}$, one gets the probability to go from $\mathbf{Y}_0$ to $\mathbf{Y}$ in time t. Thus, we can write the quantity P, introduced above, as

$$P(\mathbf{Y},\mathbf{Y}_0;t)=\int_{\mathcal{C}} d\mathbf{R}_2 d\mathbf{R}_1 \tilde{P}(\mathbf{Y},\mathbf{R}_2;t-t_2) \times \tilde{P}(\mathbf{R}_2,\mathbf{R}_1;t_2-t_1)P(\mathbf{R}_1,\mathbf{Y}_0;t_1), \quad (25)$$

where $\tilde{P}(\mathbf{R}_2,\mathbf{R}_1;t)$ is the probability density to go from $\mathbf{R}_1$ to $\mathbf{R}_2$ in time t, but $P(\mathbf{R}_1,\mathbf{Y}_0;t)$ is a probability density multiplied by the injection momentum $p_F\cos\theta_0$.

Since we are only interested in paths that have an intersection as small crossing angle, ϵ, we can restrict the probabilities inside the integral to such paths by defining $\mathbf{R}_1$ ($\mathbf{R}_2$) as the phase-space position for the first (second) visit to the crossing occurring at time t_1 (t_2). We can then write $d\mathbf{R}_2=v_F^2\sin\epsilon dt_1 dt_2 d\epsilon$ and set $\mathbf{R}_2\equiv(\mathbf{r}_2,\phi_2)=(\mathbf{r}_1,\phi_1\pm\epsilon)$. Now, we note that the loop cannot close before the path segments have diverged to a distance of order of the system size L. When closer than this, the two paths leaving an encounter have hyperbolic relative dynamics, and the probability of forming a loop is zero. Hence, the duration of the loop must exceed

$$T_L(\epsilon)=\lambda^{-1}\ln[\epsilon^{-2}], \quad (26)$$

This means that the probability that a path starting at $\mathbf{Y}_0$ crosses itself at an angle $\pm\epsilon$ and then goes to lead m, multiplied by its injection momentum $p_F\cos\theta_0$, is

$$I_m(\mathbf{Y}_0,\epsilon)=2v_F^2\sin\epsilon\int_{T_L+T_W}^{\infty}dt\int_{T_L+T_W/2}^{t-T_W/2}dt_2\int_{T_W/2}^{t_2-T_L}dt_1\int_m \times d\mathbf{Y}\int_{\mathcal{C}} d\mathbf{R}_1\tilde{P}(\mathbf{Y},\mathbf{R}_2;t-t_2) \times \tilde{P}(\mathbf{R}_2,\mathbf{R}_1;t_2-t_1)P(\mathbf{R}_1,\mathbf{Y}_0;t_1), \quad (27)$$

where the $\mathbf{Y}$ integral is over the cross section of the mth lead, and T_W and T_L are shorthand for $T_W(\epsilon)$ and $T_L(\epsilon)$.

To get g^{wl0}, we sum only contributions where $\gamma 1$ crosses itself; we then take twice the real part of this result to include the contributions where $\gamma 1$ avoids the crossing (and hence $\gamma 2$ crosses itself). Thus,

$$g_{mm_0}^{\mathrm{wl0}}=(\pi\hbar)^{-1}\int_{m_0}d\mathbf{Y}_0\int_0^{\infty}d\epsilon\,\mathrm{Re}[e^{i\delta S_{\mathrm{wl}}/\hbar}]\langle I_m(\mathbf{Y}_0,\epsilon)\rangle. \quad (28)$$

To average $I_m(\mathbf{Y}_0,\epsilon)$, we have to consider the average behavior of the P's. Within $T_W(\epsilon)/2$ of the crossing, the two legs of a self-intersecting path have a joint survival probability given by Eq. (13), since they are exploring the same region of phase space. Elsewhere, the paths' survival probability is given by Eq. (10), because there they are exploring different region of phase space. As a result, the survival probability of a self-intersecting path of length $t>T_W+T_L$ is $\exp[-(t-2T_W)/\tau_{D1}-T_W/\tau_{D2}]$. Since $\tau_{D2}^{-1}\leqslant 2\tau_{D1}^{-1}$, self-intersecting paths have an enhanced survival probability compared to noncrossing paths of the same length. When the tunnel barriers are absent, we have $\tau_{D2}=\tau_{D1}$ and the survival probability is $\exp[-(t-T_W)/\tau_{D1}]$, as in Refs. 18 and 20 and as first noted in Ref. 16. Outside the correlated region, the legs can

escape independently at any time through either lead. It is natural to assume that the probability density for the path to go to a given point in phase space is uniform. In this case, the probability density for leg 1 (including the tunneling into the cavity from lead m_0) gives

$$\langle P(\mathbf{R}_1,\mathbf{Y}_0;t_1)\rangle = \rho_{m_0} p_F \cos\theta_0 \frac{\exp[-(t_1 - T_W/2)/\tau_{D1} - T_W/(4\tau_{D2})]}{2\pi A}, \quad (29)$$

the loop's probability density is

$$\langle \tilde{P}(\mathbf{R}_2,\mathbf{R}_1;t_2 - t_1)\rangle = \frac{\exp[-[t_2 - t_1 - T_W/2]/\tau_{D1} - T_W/(2\tau_{D2})]}{2\pi A}, \quad (30)$$

and the probability density for leg 2 (including tunneling into lead m) is

$$\langle \tilde{P}(\mathbf{Y},\mathbf{R}_2;t - t_2)\rangle = \rho_m \frac{\cos\theta \exp[-(t - t_2 - T_W/2)/\tau_{D1} - T_W/(4\tau_{D2})]}{2\tau_{D1}\sum_{m'} \rho_{m'} W_{m'}}. \quad (31)$$

Note that all the above probabilities are *conditional* on the fact the path has an encounter, so that the pair of path segments within $T_W/2$ of that encounter has a joint survival probability given by Eq. (13) (for convenience, we divide that joint survival probability equally between the path segments). Thus, we find that

$$\langle \tilde{P}(\mathbf{Y},\mathbf{R}_2;t - t_2)\tilde{P}(\mathbf{R}_2,\mathbf{R}_1;t_2 - t_1)P(\mathbf{R}_1,\mathbf{Y}_0;t_1)\rangle = \frac{\rho_{m_0}\rho_m}{(2\pi A)^2} \frac{p_F \cos\theta \cos\theta_0}{2\tau_{D1}\sum_{m'} \rho_{m'} W_{m'}} \exp[-(t - 2T_W)/\tau_{D1} - T_W/\tau_{D2}], \quad (32)$$

so that $\langle I_m(\mathbf{Y}_0,\epsilon)\rangle$ becomes

$$\langle I_m(\mathbf{Y}_0,\epsilon)\rangle = \frac{\rho_{m_0}\rho_m (v_F\tau_{D1})^2}{\pi A} \frac{N_m p_F \sin\epsilon \cos\theta_0}{\sum_{m'} \rho_{m'} N_{m'}} \exp[-T_W/\tau_{D2} - (T_L - T_W)/\tau_{D1}]. \quad (33)$$

We insert this into Eq. (28). The integral over ϵ is dominated by contributions with $\epsilon \ll 1$, so that we write $\sin\epsilon \simeq \epsilon$ and push the upper bound for the ϵ integration to infinity. Then, the integral over ϵ is[14]

$$\mathrm{Re}\left[\int_0^\infty \epsilon d\epsilon (L\epsilon/W)^{2/(\lambda\tau_{D2})} \exp\left[\frac{iE_F\epsilon^2}{\lambda\hbar}\right]\right] = \frac{\lambda\hbar}{2E_F} \mathrm{Re}[i^{1+(\lambda\tau_{D2})^{-1}}]\Gamma[1 + (\lambda\tau_{D2})^{-1}]\left(\frac{\lambda\hbar L^2}{E_F W^2}\right)^{(\lambda\tau_{D2})^{-1}} = -\frac{\pi\hbar}{2mv_F^2\tau_{D2}} \exp[-\tau_E^{\mathrm{op}}/\tau_{D2}] + \mathcal{O}[(\lambda\tau_{D2})^{-1}], \quad (34)$$

where to get the second line we expanded to leading order in $(\lambda\tau_{D2})^{-1}$; in this situation, the Euler gamma function $\Gamma[1+(\lambda\tau_{D2})^{-1}] \simeq 1$. Note that when we neglect all $\mathcal{O}[(\lambda\tau_{D2})^{-1}]$ corrections, this must include all terms of order one in the logarithm of the Ehrenfest time, since they can only lead to $\mathcal{O}[(\lambda\tau_{D2})^{-1}]$ corrections to the above expression. Thus, since $\lambda \sim v_F/L$, we are justified in writing $\tau_E^{\mathrm{op}} = \lambda^{-1} \ln[E_F W^2/(\lambda\hbar L^2)]$.

Note that the second term in the exponent of Eq. (33) is independent of ϵ; thus, only τ_{D2} enters the ϵ integral. The $\mathbf{Y}_0$ integral generates a factor of $2W_{m_0}$. We can write $N_m = (\pi\hbar)^{-1} p_F W_m$ and $(\Sigma_{m'}\rho_{m'}N_{m'})^{-1} = (mA)^{-1}\hbar\tau_{D1}$. Thus, the usual weak-localization contribution is

$$g_{mm_0}^{\mathrm{wl0}} = -\frac{\rho_m\rho_{m_0}N_m N_{m_0}}{\left[\sum_{m'} \rho_{m'}N_{m'}\right]^2} \frac{\tau_{D1}}{\tau_{D2}} \exp[-\tau_E^{\mathrm{op}}/\tau_{D2} - (\tau_E^{\mathrm{cl}} - \tau_E^{\mathrm{op}})/\tau_{D1}], \quad (35)$$

where τ_{D1} and τ_{D2} are given in Eqs. (11) and (14). When the tunnel barriers are transparent ($\rho_m = 1$ for all m), this is the only contribution to weak localization for $m \neq m_0$; in this case, $\tau_{D2} = \tau_{D1}$ and we get the expected result.[16,18,20]

Note that in the universal limit ($\tau_E^{\mathrm{op}} \to 0$), this contribution to conductance behaves like the naive argument given in Sec. I would predict. It goes like the weak-localization contribution to conductance for a cavity with *no* tunnel barriers and each lead having N_i' modes, where $N_i' = \rho_i N_i$ (with τ_{D1}/τ_{D2} being just a numerical prefactor with $1 \leqslant \tau_{D1}/\tau_{D2} \leqslant 2$). Hence, in the limit of opaque barriers ($\rho_m \to 0$ for all m), this contribution does not vanish for fixed Drude conductance ($\rho_m N_m$ remains constant for all m). Thus, the origin of the suppression of weak localization in the opaque limit is elsewhere.

B. Successful coherent backscattering

The coherent-backscattering contribution to transport has long been considered in trajectory-based semiclassics.[5,29] However, until recently, the approximations were a little simplistic and failed to capture the full nature of this contribution (in particular, its Ehrenfest time dependence). This was addressed in Refs. 18 and 19 in the absence of tunnel barriers. Here we perform a calculation similar to Ref. 18 while adding tunnel barriers on the leads. The coherent-backscattering contributions in the presence of these barriers are shown in Fig. 4, with Fig. 5 showing the paths in the correlated region in more detail. We treat these contributions separately from those in the previous section because injection and exit positions and momenta are correlated. These contributions are exactly those that were ignored in the previous section, paths where one and/or both legs escape within $T_W/2$ of the encounter. However, it is convenient to parametrize these contributions in terms of $(r_{0\perp}, p_{0\perp})$ instead of (ϵ, t_1).

Here, we consider the successful coherent backscattering (cbs0), the second contribution shown in Fig. 4. This successful contribution gives the coherent backscattering when the tunnel barriers are absent ($\rho_m = 1$ for all m). From Ref. 18, we have that

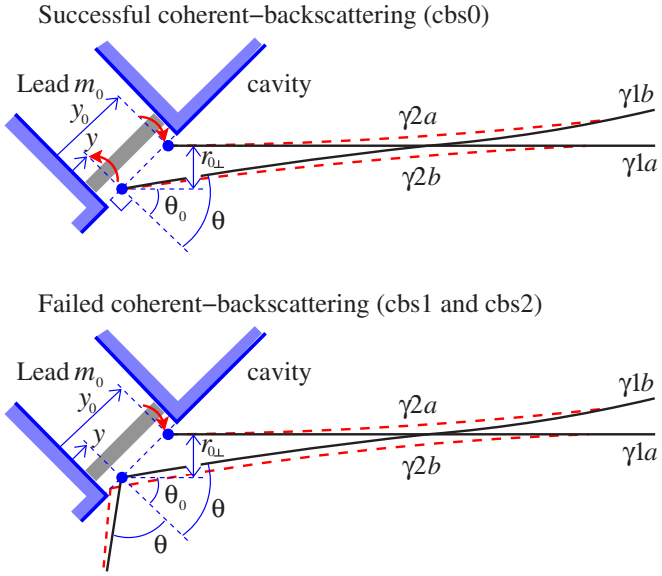

FIG. 5. (Color online) Details of the paths that contribute to successful and failed coherent backscatterings (cbs0, cbs1, and cbs2). Path $\gamma 1$ (solid black line) start on the cross section of lead m_0 at position y_0 with momentum angle θ_0 and returns at y with momentum angle θ. For the successful contribution, it then tunnels into the lead; for the failed contribution, it is reflected off the barrier and remains in the chaotic system. All paths are drawn in the basis parallel and perpendicular to $\gamma 1$ at injection; the initial position and momentum of path $\gamma 1$ at exit are $r_{0\perp}=(y_0-y)\cos\theta_0$, $r_{0\parallel}=(y_0-y)\sin\theta_0$, and $p_{0\perp}\simeq -p_F(\theta-\theta_0)$.

$$S_{2b}-S_{1a}=p_F r_{0\parallel}+\tfrac{1}{2}m\lambda r_{0\perp}^2, \tag{36}$$

$$S_{2a}-S_{1b}=-p_F r_{0\parallel}+p_{0\perp}r_{0\perp}+\tfrac{1}{2}m\lambda r_{0\perp}^2, \tag{37}$$

where $(r_{0\perp},p_{0\perp})$ are the position and momentum of path segment $\gamma 1b$ relative to path segment $\gamma 1a$, shown in Fig. 5. Thus, the total action difference between these two paths is

$$\delta S_{\mathrm{cbs0}}=(p_{0\perp}+m\lambda r_{0\perp})r_{0\perp}. \tag{38}$$

The successful coherent-backscattering contribution to the reflection is

$$g_{mm_0}^{\mathrm{cbs0}}=\delta_{mm_0}(2\pi\hbar)^{-2}\int_{m_0}d\mathbf{Y}_0 d\mathbf{Y}\int_0^\infty dt\langle P(\mathbf{Y},\mathbf{Y}_0;t)\rangle \times \mathrm{Re}[e^{i\delta S_{\mathrm{cbs0}}/\hbar}], \tag{39}$$

where δ_{mm_0} is a Kronecker δ function.

To perform the average, we define $T'_W(r_{0\perp},p_{0\perp})$ and $T'_L(r_{0\perp},p_{0\perp})$ as the times between touching the tunnel barrier and the perpendicular distance between $\gamma 1a$ and $\gamma 1b$ becoming W and L, respectively. For times less than $T'_W(r_{0\perp},p_{0\perp})$, the path segments ($\gamma 1a$ and $\gamma 1b$) are paired; thus, their joint survival probability is given by Eq. (13). For times longer than this, the path segments escape independently, so each has a survival probability given by Eq. (10). For $g_{mm_0}^{\mathrm{cbs0}}$, we consider only those paths that form a closed loop; however, they cannot close until the two path segments are of order of L apart. This means that the t integral in Eq. (39) must have a lower cutoff at $2T'_L(r_{0\perp},p_{0\perp})$; hence, we have

$$\int_{m_0}d\mathbf{Y}\int_{2T'_L}^\infty dt\langle P(\mathbf{Y},\mathbf{Y}_0;t)\rangle = \rho_{m_0}^2 p_F\cos\theta_0\frac{N_{m_0}}{\sum_{m'}\rho_{m'}N_{m'}}\exp[-T'_W/\tau_{D2}-2(T'_L-T'_W)/\tau_{D1}], \tag{40}$$

where $T'_{L,W}$ are shorthand for $T'_{L,W}(r_{0\perp},p_{0\perp})$. For small $(p_{0\perp}+m\lambda r_{0\perp})$, we estimate[33]

$$T'_W(r_{0\perp},p_{0\perp})\simeq\lambda^{-1}\ln\left[\frac{m\lambda W}{|p_{0\perp}+m\lambda r_{0\perp}|}\right], \tag{41}$$

$$T'_L(r_{0\perp},p_{0\perp})\simeq\lambda^{-1}\ln\left[\frac{m\lambda L}{|p_{0\perp}+m\lambda r_{0\perp}|}\right]. \tag{42}$$

Thus, $(T'_L-T'_W)$ is independent of $(r_{0\perp},p_{0\perp})$; indeed, $2(T'_L-T'_W)=(\tau_E^{\mathrm{cl}}-\tau_E^{\mathrm{op}})$. We substitute the above expressions into $g_{mm_0}^{\mathrm{cbs0}}$, write[29] $p_F\cos\theta_0 d\mathbf{Y}_0=dy_0 d(p_F\sin\theta_0)=dr_{0\perp}dp_{0\perp}$, and then make the substitution $\tilde{p}_0=p_{0\perp}+m\lambda r_{0\perp}$. We evaluate the $r_{0\perp}$ integral over a range of order W_{m_0}. Then, taking the limits on the resulting $\tilde{p}_0$ integral to infinity, it takes the form

$$\int_{-\infty}^\infty d\tilde{p}_0\frac{2\hbar\sin(\tilde{p}_0W/\hbar)}{\tilde{p}_0}\left|\frac{\tilde{p}_0}{m\lambda W}\right|^{1/(\lambda\tau_{D2})} = \frac{4\hbar}{(m\lambda W)^{1/(\lambda\tau_{D2})}}\mathrm{Im}\left[\int_0^\infty d\tilde{p}_0\tilde{p}_0^{-1+1/(\lambda\tau_{D2})}\exp[i\tilde{p}_0W/\hbar]\right] = 2\pi\hbar\left(\frac{\hbar}{m\lambda W^2}\right)^{1/(\lambda\tau_{D2})}. \tag{43}$$

To evaluate the integral, we wrote it in terms of an Euler Γ function. Note that $[\hbar/(m\lambda W^2)]^{1/(\lambda\tau_{D2})}\simeq\exp[-\tau_E^{\mathrm{op}}/\tau_{D2}]$ once we have dropped $\mathcal{O}(1)$ terms inside the logarithm. The result is that

$$g_{mm_0}^{\mathrm{cbs0}}=\delta_{mm_0}\frac{\rho_{m_0}^2N_{m_0}}{\sum_{m'}\rho_{m'}N_{m'}}\exp[-\tau_E^{\mathrm{op}}/\tau_{D2}-(\tau_E^{\mathrm{cl}}-\tau_E^{\mathrm{op}})/\tau_{D1}]. \tag{44}$$

This successful coherent-backscattering contribution has exactly the same exponential dependence on τ_E^{op} and τ_E^{cl} as the usual weak localization. This must be the case if the theory is to preserve unitarity (conserve current); however, since wl0 and cbs0 were calculated separately using different methods, this acts as a check on our algebra.

C. Failed coherent backscattering

Here, we consider the failed coherent backscattering (cbs1 and cbs2), see Figs. 4(c) and 4(d). We call them *failed* contributions because they are part of the coherent-backscattering peak for the chaotic system; however, they are reflected back into the cavity by the tunnel barriers. They can

then contribute to either transmission or reflection.

The action difference for coherent-backscattering paths that reflect at the barrier is slightly different from that for the paths that transmit. This is because the path segments $\gamma 1b$ and $\gamma 2b$ converge at infinity rather than at the lead (see Fig. 5). We split path segment $\gamma 1b$ into $\gamma 1b'$ before the failure to tunnel and $\gamma 1b''$ after the failure to tunnel. We do the same for path segment $\gamma 2b$. Then the action difference is the sum of three terms. The first two come from before the failed tunneling; they are

$$S_{2b'} - S_{1a} = p_F r_{0\|} + (m\lambda/8)[r_{0\perp} - p_{0\perp}/(m\lambda)]^2, \quad (45)$$

and $(S_{2a}-S_{1b'})$ still given by Eq. (37). The third term is the action difference of path segments after the failure to tunnel,

$$S_{2b''} - S_{1b''} = -p_{0\perp}[r_{0\perp} + p_{0\perp}/(m\lambda)] + (m\lambda/2)[r_{0\perp} + p_{0\perp}/(m\lambda)]^2, \quad (46)$$

Hence, the total action difference between the two paths is

$$\delta S_{\mathrm{cbs1}} = \delta S_{\mathrm{cbs0}} + \tilde{p}_0^2/(4m\lambda), \quad (47)$$

where we write $\tilde{p}_0 = p_{0\perp} + m\lambda r_{0\perp}$ and hence $\delta S_{\mathrm{cbs0}} = r_{0\perp}\tilde{p}_0$, as in Sec. V B. As before, we evaluate the integral over $r_{0\perp}$ first, getting an integral for $\tilde{p}_0$ of the form

$$\int_{-\infty}^{\infty} d\tilde{p}_0 \frac{2\hbar \sin(\tilde{p}_0 W/\hbar)}{\tilde{p}_0} \exp\left[\frac{i\tilde{p}_0^2}{4m\lambda\hbar}\right] \left|\frac{\tilde{p}_0}{m\lambda W}\right|^{1/(\lambda\tau_{D2})} = 2\pi\hbar\left(\frac{\hbar}{m\lambda W^2}\right)^{1/(\lambda\tau_{D2})}. \quad (48)$$

To get this result, we noted that $p_0 \lesssim \hbar/W$ in the region which dominates the integral, so we approximated $\exp[i\tilde{p}_0^2(4m\lambda\hbar)^{-1}]=1$; after this the integral is identical to Eq. (43).

For the first failed backscattering contribution (cbs1), the bulk of the derivation is identical to that of the successful coherent backscattering (cbs0) above. The difference here is that at the point where the path returns to the lead, it is reflected from the barrier (with probability $1-\rho_{m_0}$) instead of being transmitted (with probability ρ_{m_0}). The path then remains in the cavity and will eventually escape through an arbitrary lead, with the probability of escape through lead m being $[\Sigma_{m'}\rho_{m'}N_{m'}]^{-1}\rho_m N_m$. Thus, we can conclude that

$$g_{mm_0}^{\mathrm{cbs1}} = g_{m_0m_0}^{\mathrm{cbs0}} \frac{1-\rho_{m_0}}{\rho_{m_0}} \frac{\rho_m N_m}{\sum_{m'} \rho_{m'}N_{m'}} = \frac{\rho_m \rho_{m_0}(1-\rho_{m_0}) N_m N_{m_0}}{\left[\sum_{m'} \rho_{m'}N_{m'}\right]^2} \times \exp[-\tau_E^{\mathrm{op}}/\tau_{D2} - (\tau_E^{\mathrm{cl}} - \tau_E^{\mathrm{op}})/\tau_{D1}]. \quad (49)$$

The second failed coherent-backscattering contribution (cbs2) can be immediately written down by swapping all subscripts m_0 with m; hence,

$$g_{mm_0}^{\mathrm{cbs2}} = \frac{\rho_m \rho_{m_0}(1-\rho_m) N_m N_{m_0}}{\left[\sum_{m'} \rho_{m'}N_{m'}\right]^2} \exp[-\tau_E^{\mathrm{op}}/\tau_{D2} - (\tau_E^{\mathrm{cl}} - \tau_E^{\mathrm{op}})/\tau_{D1}]. \quad (50)$$

For $m=m_0$, one must confirm that cbs1 and cbs2 are not double counting the same contribution. One can see that they form different contributions from the fact that one starts with a leg (two paths identical) and ends with a loop (two paths nonidentical), while the other starts with the loop and ends with a leg.

D. The total weak-localization correction with tunnel barriers

We sum the contributions calculated in the preceding sections, Eqs. (35), (44), (49), and (50), and get

$$g_{mm_0}^{\mathrm{wl}} = -\frac{\rho_m \rho_{m_0} N_m N_{m_0}}{\left[\sum_{m'} \rho_{m'}N_{m'}\right]^2} \mathcal{A}_{mm_0} \exp[-\tau_E^{\mathrm{op}}/\tau_{D2} - (\tau_E^{\mathrm{cl}} - \tau_E^{\mathrm{op}})/\tau_{D1}], \quad (51)$$

where we define

$$\mathcal{A}_{mm_0} \equiv \rho_m + \rho_{m_0} - \frac{\sum_{m'} \rho_{m'}^2 N_{m'}}{\sum_{m'} \rho_{m'}N_{m'}} - \frac{\delta_{mm_0}}{N_{m_0}} \sum_{m'} \rho_{m'}N_{m'}, \quad (52)$$

with δ_{mm_0} being a Kronecker δ function. Note that $\mathcal{A}$ goes like $(\rho \times N^0)$. Thus, in the limit $\rho \to 0$ with constant ρN, we see that $\mathcal{A} \to 0$ and the weak-localization contribution to conductance goes to zero.

As a check on our result, we verify that $\Sigma_m g_{mm_0}^{\mathrm{wl}} = 0$; this means that we have not violated unitarity (or current conservation).

Finally, we consider the special case of two leads (L and R) with barriers with tunnel probability $\rho_{\mathrm{L,R}}$ and number of modes $N_{\mathrm{L,R}}$, and then we find that Eq. (51) reduces to

$$\delta g_{\mathrm{LR}}^{\mathrm{wl}} = -\frac{\rho_{\mathrm{L}}^2 \rho_{\mathrm{R}}^2 N_{\mathrm{L}} N_{\mathrm{R}} (N_{\mathrm{L}} + N_{\mathrm{R}})}{(\rho_{\mathrm{L}} N_{\mathrm{L}} + \rho_{\mathrm{R}} N_{\mathrm{R}})^3} \exp[-\tau_E^{\mathrm{op}}/\tau_{D2} - (\tau_E^{\mathrm{cl}} - \tau_E^{\mathrm{op}})/\tau_{D1}], \quad (53)$$

with $\delta g_{\mathrm{LL}}^{\mathrm{wl}} = \delta g_{\mathrm{RR}}^{\mathrm{wl}} = -\delta g_{\mathrm{RL}}^{\mathrm{wl}} = -\delta g_{\mathrm{LR}}^{\mathrm{wl}}$.

VI. SHOT NOISE FOR A CHAOTIC SYSTEM WITH TUNNEL BARRIERS

Now, we turn to the zero-frequency shot-noise power S for quantum chaotic systems. This intrinsically quantum part of the fluctuations of a nonequilibrium electronic current often contains information on the system that cannot be obtained through conductance measurements. We give our results in terms of the Fano factor $F=S/S_P$, which is the ratio of S to the Poissonian noise $S_P=2e\langle I\rangle$ that would be generated by a current flow of uncorrelated particles. Alternatively, one can think of the Fano factor as the ratio of the noise to the average current, written in convenient dimensionless units. According to the scattering theory of transport, one has[34]

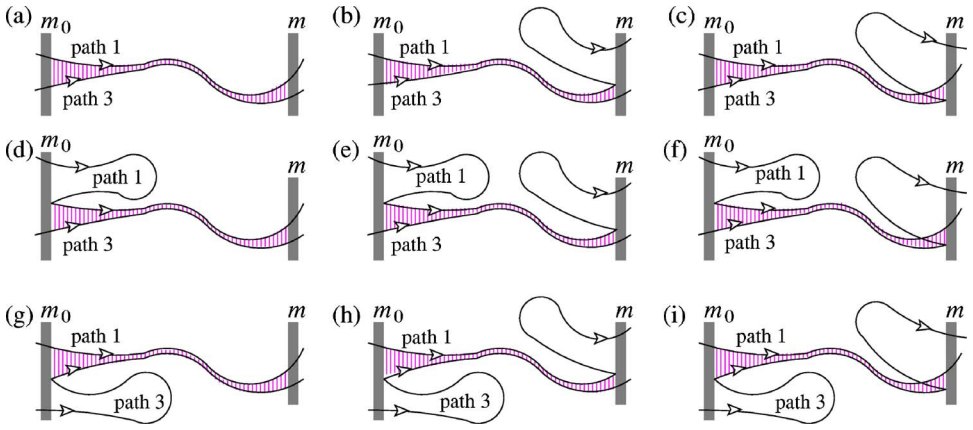

FIG. 6. (Color online) The set of contributions to $\mathrm{Tr}[\mathrm{S}^{\dagger}_{mm_0}\mathrm{S}_{mm_0}\mathrm{S}^{\dagger}_{mm_0}\mathrm{S}_{mm_0}]$ which we call $D_{1a},\ldots,D_{1i}$. These are the contributions which do not vanish for infinite Ehrenfest time. Here, we show only the tunnel barriers on leads m_0 and m as shaded rectangles; a path which crosses the barrier on lead m has succeeded in tunneling out of the cavity into the lead. The contributions are made up of four classical paths; here, we show only two of the paths (1 and 3). The other two paths (2 and 4) look the same as the paths shown, *except* that they cross at the center of the correlated region (indicated by the vertical cross hatching). In the correlated region, the paths have the same topology as shown in Fig. 3 if we replace the labels in the manner given in Eq. (58). Thus, path 4 is paired with path 1 at lead m_0 but paired with path 3 at lead m (and vice versa for path 2). The noise in these contribution is purely due to the stochastic nature of scattering at the tunnel barriers; if they were absent, these contributions would be noiseless. The calculation will show that all these contributions go like $(1-e^{-\tau_E^{\mathrm{op}}/\tau_{D2}})$.

$$F = \frac{\mathrm{Tr}[\mathrm{S}^{\dagger}_{mm_0}\mathrm{S}_{mm_0}] - \mathrm{Tr}[\mathrm{S}^{\dagger}_{mm_0}\mathrm{S}_{mm_0}\mathrm{S}^{\dagger}_{mm_0}\mathrm{S}_{mm_0}]}{\mathrm{Tr}[\mathrm{S}^{\dagger}_{mm_0}\mathrm{S}_{mm_0}]}. \qquad (54)$$

We use the trajectory-based method developed in Ref. 17 to evaluate the contributions to this quantity to lowest order in N^{-1}, where N is the number of lead modes. We thereby neglect all the weak-localization-type corrections to the noise calculated in Ref. 8. At this order, all contributions are listed in Figs. 6 and 7. The contributions fall naturally into two classes. The first class, shown in Fig. 6, involves classical paths (paths 1 and 3) which are correlated, and one or both paths escape *before* their flow under the cavity dynamics makes them become uncorrelated. The second class, shown in Fig. 7, involve correlated paths which become uncorrelated under the cavity's classical dynamics before any paths escape. As before, *uncorrelated* means that the paths are almost parallel and within W of each other.

The denominator and the first term in the numerator of Eq. (54) are equal to the Drude conductance and are hence given by Eq. (22) with $m \neq m_0$. Thus, to find the Fano factor, we must evaluate $\mathrm{Tr}[\mathrm{S}^{\dagger}_{mm_0}\mathrm{S}_{mm_0}\mathrm{S}^{\dagger}_{mm_0}\mathrm{S}_{mm_0}]$. As with weak localization, we approximate $\Sigma_n\langle y'|n\rangle\langle n|y\rangle \approx \delta(y'-y)$, then it becomes a sum over four paths, $\gamma 1$ from y_{01} to y_1, $\gamma 2$ from y_{03} to y_1, $\gamma 3$ from y_{03} to y_3, and $\gamma 4$ from y_{01} to y_3, where y_{01} and y_{03} are on lead m_0 and y_1 and y_3 are on lead m. Hence,

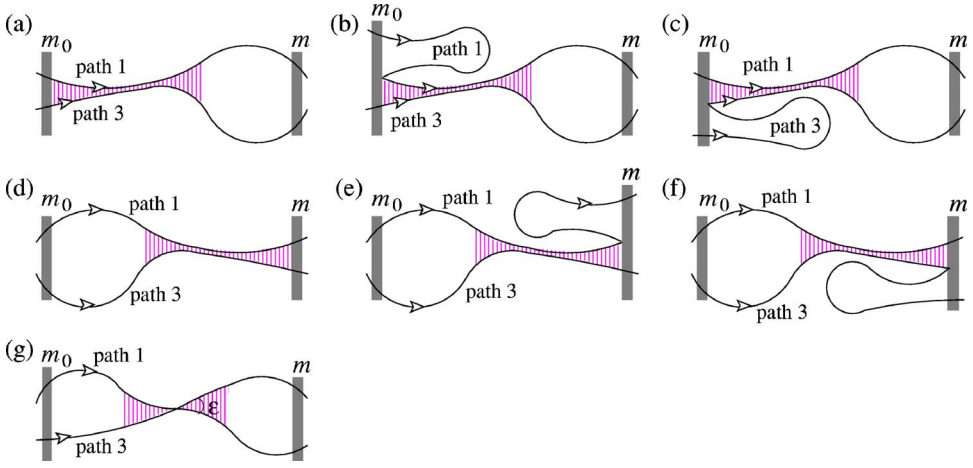

FIG. 7. (Color online) The set of contributions to $\mathrm{Tr}[\mathrm{S}^{\dagger}_{mm_0}\mathrm{S}_{mm_0}\mathrm{S}^{\dagger}_{mm_0}\mathrm{S}_{mm_0}]$ which we call $D_{2a},\ldots,D_{2g}$. These are the contributions which vanish for infinite Ehrenfest time. The contributions are drawn in the same manner as Fig. 6, with only paths 1 and 3 shown. As before, paths 2 and 4 are equivalent to 1 and 3 except that they cross at the center of the correlated region (indicated by vertical cross hatching). For finite Ehrenfest times, the paths must escape the correlated region (vertical cross hatching) before either tunnels out of the cavity (on at least one side of the encounter). The calculation will show that all these contributions go like $e^{-\tau_E^{\mathrm{op}}/\tau_{D2}}$.

$$\mathrm{Tr}[\mathrm{S}^{\dagger}_{mm_0}\mathrm{S}_{mm_0}\mathrm{S}^{\dagger}_{mm_0}\mathrm{S}_{mm_0}] = \frac{1}{(2\pi\hbar)^2}\int_{\mathrm{L}} dy_{01}dy_{03}\int_{\mathrm{R}} dy_1 dy_3 \times \sum_{\gamma 1,\ldots,\gamma 4} A^{*}_{\gamma 4}A_{\gamma 3}A^{*}_{\gamma 2}A_{\gamma 1}\exp[\mathrm{i}\delta S/\hbar], \quad (55)$$

where A_γ is given by Eq. (17), and $\delta S = S_{\gamma 1} - S_{\gamma 2} + S_{\gamma 3} - S_{\gamma 4}$ (we have absorbed all Maslov indices into the actions $S_{\gamma i}$). The dominant contributions that survive averaging over energy or cavity shape are those for which the fluctuations of $\delta S/\hbar$ are minimal. They are shown in Figs. 6 and 7. Their paths are in pairs almost everywhere except in the vicinity of encounters. Going through an encounter, two of the four paths cross each other, while the other two avoid the crossing. They remain in pairs, though the pairing switches, e.g., from $(\gamma 1;\gamma 4)$ and $(\gamma 2;\gamma 3)$ to $(\gamma 1;\gamma 2)$ and $(\gamma 3;\gamma 4)$. Paths are always close enough to their partner that their stability is the same. Thus, for all pairings,

$$\sum_{\gamma 1,\ldots,\gamma 4} A^{*}_{\gamma 4}A_{\gamma 3}A^{*}_{\gamma 2}A_{\gamma 1} \to \sum_{\gamma 1,\gamma 3} |A_{\gamma 3}|^2|A_{\gamma 1}|^2. \quad (56)$$

Then the sum over all paths γ from y_0 to y is given by Eq. (20). As with weak localization, we define $P(\mathbf{Y},\mathbf{Y}_0;t)\delta y\delta\theta\delta t$ as the product of the momentum along the injection lead, $p_F\cos\theta_0$, and the classical probability to go from an initial position and angle $\mathbf{Y}_0=(y_0,\theta_0)$ to within $(\delta y,\delta\theta)$ of $\mathbf{Y}$ in a time within δt of t. We remind the reader that this probability is to go from the injection lead to the exit lead, and this includes the tunneling probability at each barrier. We now use Eqs. (20), (55), and (56) to analyze the contributions in Figs. 6 and 7. All contributions can be written as

$$D_i = \frac{1}{(2\pi\hbar)^2}\int_{\mathrm{L}} d\mathbf{Y}_{01}d\mathbf{Y}_{03}\int_{\mathrm{R}} d\mathbf{Y}_1 d\mathbf{Y}_3\int dt_1 dt_3 \times\langle P(\mathbf{Y}_1,\mathbf{Y}_{01};t_1)P(\mathbf{Y}_3,\mathbf{Y}_{03};t_3)\rangle\exp[\mathrm{i}\delta S_{D_i}/\hbar], \quad (57)$$

where the subscripts 1 and 3 indicate paths 1 and 3, respectively. When evaluating Eq. (57), the joint exit probability for two crossing paths has to be computed.

A. Noise contributions which do not vanish for infinite Ehrenfest time

To evaluate all the contributions in Fig. 6, we note that the paths never become uncorrelated under the classical dynamics; they only escape in an uncorrelated manner if one path tunnels while the other is reflected. In this case, the details of the encounter are as given in Fig. 5, if we make the replacements

$$\text{path segment } \gamma 1a \to \text{path } \gamma 1,$$
$$\text{path segment } \gamma 2a \to \text{path } \gamma 2,$$
$$\text{path segment } \gamma 1b \to \text{path } \gamma 3,$$
$$\text{path segment } \gamma 2b \to \text{path } \gamma 4. \quad (58)$$

Thus, the action difference between the paths can be evaluated in a manner equivalent to coherent backscattering. For contributions where the paths escape while correlated, the action difference is given by $\delta S_{D_i}=\delta S_{\mathrm{cbs0}}$, where δS_{cbs0} is given in Eq. (38). For contributions where the correlation is broken by some of the paths escaping, the action difference is given by $\delta S_{D_i}=\delta S_{\mathrm{cbs1}}$, with δS_{cbs1} given in Eq. (47). Here, as in Sec. V C, the difference between δS_{cbs1} and δS_{cbs0} has no effect on the final result, so one could just use δS_{cbs0} for all contributions.

For the contribution in Fig. 6(a), the paths paired at lead m_0 remain paired at lead m; thus, the length of the paired paths must be less than $T'_W(r_{0\perp},p_{0\perp})$ given in Eq. (41). Thus, we see that

$$\int_m d\mathbf{Y}_1 d\mathbf{Y}_3\int_0^{T'_W} dt_1 dt_3\langle P(\mathbf{Y}_1,\mathbf{Y}_{01};t_1)P(\mathbf{Y}_3,\mathbf{Y}_{03};t_3)\rangle = \frac{\rho_m^2 N_m p_F^2\cos\theta_{01}\cos\theta_{03}}{\sum_{m'}\rho_{m'}(2-\rho_{m'})N_{m'}}(1-\exp[-T'_W/\tau_{D2}]), \quad (59)$$

where T'_W is the function of $(r_{0\perp},p_{0\perp})$ given in Eq. (41). Note that the denominator comes from the fact that we are considering the survival probability for correlated paths; thus, the probability that the correlation is destroyed by paths escaping into a lead during the time t to $t+\delta t$ is $P_2(t)\times\delta t/\tau_{D2}$, where $P_2(t)$ is given by Eq. (13). We insert Eq. (59) into Eq. (57), and then just as in Sec. V B, we change integration variables using $p_F\cos\theta_{03}d\mathbf{Y}_{03} = dr_{0\perp}dp_{0\perp}$ and define $\tilde{p}_0\equiv p_{0\perp}+m\lambda r_{0\perp}$. In the regime of interest, $T'_W(r_{0\perp},p_{0\perp})\simeq\lambda^{-1}\ln[m\lambda W/|\tilde{p}_0|]$. Evaluating the integral over $r_{0\perp}$ leaves a $\tilde{p}_0$ integral which we cast as an Euler Γ function, just as for coherent backscattering in Sec. V B. To lowest order in $(\lambda\tau_{D2})^{-1}$, we find that the contribution to $\mathrm{Tr}[\mathrm{S}^{\dagger}_{mm_0}\mathrm{S}_{mm_0}\mathrm{S}^{\dagger}_{mm_0}\mathrm{S}_{mm_0}]$ shown in Fig. 6(a) is

$$D_{1\mathrm{a}} = \frac{\rho_{m_0}^2\rho_m^2 N_{m_0}N_m(1-\exp[-\tau_E^{\mathrm{op}}/\tau_{D2}])}{\sum_{m'}\rho_{m'}(2-\rho_{m'})N_{m'}}. \quad (60)$$

Now, we note that each contribution in Fig. 6 is of a similar form to $D_{1\mathrm{a}}$. For example, $D_{1\mathrm{b}}$ and $D_{1\mathrm{c}}$ are like $D_{1\mathrm{a}}$ with the exception that a path is reflected off lead m and then returns to lead m. The result of the integral over $(r_{0\perp},p_{0\perp})$ is basically unchanged when we replace the action difference in Eq. (38) with Eq. (47), see Sec. V C. Thus, we get each of these contributions by simply multiplying $D_{1\mathrm{a}}$ by

$$\frac{1-\rho_m}{\rho_m}\frac{\rho_m N_m}{\sum_{m'}\rho_{m'}N_{m'}} = \frac{(1-\rho_m)N_m}{\sum_{m'}\rho_{m'}N_{m'}}, \quad (61)$$

where after reflection the path that remains in the cavity evolves alone, so its survival is governed by Eq. (10). We can make the same argument for paths which enter the cavity from lead m_0 at different times, but in such a way that the

second enters the cavity at a moment when by chance the first is reflecting off barrier m_0 in such a way that the paths form a pair. To make the argument, we need to simply reverse the direction of the paths, and we return to the situation discussed above Eq. (61) with m replaced by m_0. Thus, we find that the sum of all contributions in Fig. 6 is

$$D_1 = \frac{\rho_{m_0}^2 \rho_m^2 N_{m_0} N_m (1 - \exp[-\tau_E^{\rm op}/\tau_{D2}])}{\sum_{m'} \rho_{m'}(2-\rho_{m'})N_{m'}} \times \left(1 + \frac{2(1-\rho_{m_0})N_{m_0}}{\sum_{m'} \rho_{m'} N_{m'}}\right)\left(1 + \frac{2(1-\rho_m)N_m}{\sum_{m'} \rho_{m'} N_{m'}}\right). \quad (62)$$

B. Noise contributions which vanish for infinite Ehrenfest time

To evaluate all the contributions in Fig. 7 except Fig. 7(g), we note that the path pairs are always correlated at one lead; at that lead, they only escape in an uncorrelated manner if one path tunnels while the other is reflected. In this case, the details of the encounter are as given in Fig. 5, if we make the replacements given in Eq. (58). These contributions are extremely similar to those discussed in Sec. VI A; the only difference is that the paths become more than the lead width apart at least one lead. This occurs because the correlated paths survive for a time longer than T_W'. Thus, for the contribution in Fig. 7(a), we have

$$\int_m d\mathbf{Y}_1 d\mathbf{Y}_3 \int_{T_W'}^{\infty} dt_1 dt_3 \langle P(\mathbf{Y}_1, \mathbf{Y}_{01}; t_1) P(\mathbf{Y}_3, \mathbf{Y}_{03}; t_3)\rangle = \frac{\rho_m^2 N_m^2 p_F^2 \cos\theta_{01} \cos\theta_{03}}{\left(\sum_{m'} \rho_{m'} N_{m'}\right)^2} \exp[-T_W'/\tau_{D2}]. \quad (63)$$

Since the paths separate inside the cavity under the classical dynamics, their escape is given by the single-path escape. However, the factor of $\exp[-T_W'/\tau_{D2}]$ is due to the fact that the correlated paths must first survive until time $T_W'(r_{0\perp}, p_{0\perp})$, and during this time, the survival probability is given by Eq. (13). Compare this with the equivalent contribution, Eq. (59), for pairs which escape on a time less than T_W'. The integral over $(r_{0\perp}, p_{0\perp})$ can be evaluated in exactly the same manner as D_{1a} (and in the same manner as the coherent backscattering in Sec. V B). Then, we find that

$$D_{2a} = \frac{\rho_{m_0}^2 \rho_m^2 N_{m_0} N_m^2 \exp[-\tau_E^{\rm op}/\tau_{D2}]}{\left(\sum_{m'} \rho_{m'} N_{m'}\right)^2}. \quad (64)$$

We then note that contributions D_{2b} and D_{2c} equal D_{2a} multiplied by $(1-\rho_{m_0})/(\Sigma_{m'}\rho_{m'}N_{m'})$; thus,

$$D_{2a} + D_{2b} + D_{2c} = \frac{\rho_{m_0}^2 \rho_m^2 N_{m_0} N_m^2 \exp[-\tau_E^{\rm op}/\tau_{D2}]}{\left(\sum_{m'} \rho_{m'} N_{m'}\right)^2} \times \left(1 + \frac{2(1-\rho_{m_0})N_{m_0}}{\sum_{m'} \rho_{m'} N_{m'}}\right). \quad (65)$$

The contributions D_{2d}, D_{2e}, and D_{2f} [shown in Figs. 7(d)–7(f)] are the same as contributions D_{2a}, D_{2b}, and D_{2c} [shown in Figs. 7(a)–7(c)] with $m_0 \leftrightarrow m$. Thus,

$$D_{2d} + D_{2e} + D_{2f} = \frac{\rho_{m_0}^2 \rho_m^2 N_m^2 N_{m_0} \exp[-\tau_E^{\rm op}/\tau_{D2}]}{\left(\sum_{m'} \rho_{m'} N_{m'}\right)^2} \times \left(1 + \frac{2(1-\rho_m)N_m}{\sum_{m'} \rho_{m'} N_{m'}}\right). \quad (66)$$

This leaves us to evaluate D_{2g}, the contribution shown in Fig. 7(g); this is different from all other noise contributions because the paths are not correlated at escape. Thus, we evaluate this contribution in a manner similar to the weak-localization contribution in Sec. V A. We use the method developed by Richter and Sieber[5] while taking into account that paths in the same region of phase space have escape probabilities given by Eq. (13). This method was first applied to shot noise in Refs. 8 and 17 in the absence of tunnel barriers. Here, we follow Ref. 17, and we write the action difference as in Eq. (24), where the crossing angle ϵ is shown in Fig. 7(g). We write

$$P(\mathbf{Y}_i, \mathbf{Y}_{0i}; t_i) = \int d\mathbf{R}_i \tilde{P}(\mathbf{Y}_i, \mathbf{R}_i; t_i - t_i') P(\mathbf{R}_i, \mathbf{Y}_{0i}; t_i'),$$

where $\tilde{P}$ is the probability for the classical path to exist (not multiplied by the injection momentum), and $\mathbf{R}_i$ is a point in the system's phase space $(\mathbf{r}_i, \phi_i)$ visited at time t_i', with ϕ_i giving the direction of the momentum. We choose $\mathbf{R}_1$ and $\mathbf{R}_3$ as the points at which the paths cross, so $\mathbf{R}_3 = (\mathbf{r}_1, \phi_1 \pm \epsilon)$ and $d\mathbf{R}_3 = v_F^2 \sin\epsilon dt_1' dt_3' d\epsilon$.

To get D_{2g}, we sum only contributions where $\gamma 1$ crosses $\gamma 3$, and we then take twice the real part of this result to include the contributions where $\gamma 1$ and $\gamma 3$ avoid crossing (and hence $\gamma 2$ and $\gamma 4$ cross). Thus,

$$D_{2g} = 2(2\pi\hbar)^{-2} \int_{\rm L} d\mathbf{Y}_{01} d\mathbf{Y}_{03} \int_0^{\pi} d\epsilon \, {\rm Re}[e^{i\delta S_{D_1}/\hbar}] \times \langle I(\mathbf{Y}_{01}, \mathbf{Y}_{03}; \epsilon)\rangle, \quad (67)$$

where δS_{D_1} is the same as $\delta S_{\rm wl}$ in Eq. (24). The function $I(\mathbf{Y}_{01}, \mathbf{Y}_{03}; \epsilon)$ is related to the probability that $\gamma 3$ crosses $\gamma 1$ at angle $\pm\epsilon$. Its average is independent of $\mathbf{Y}_{01,03}$, so $\langle I(\mathbf{Y}_{01}, \mathbf{Y}_{03}; \epsilon)\rangle = \langle I(\epsilon)\rangle$. Injections and/or escapes are more than $T_W(\epsilon)/2$ from the crossing, so

$$\langle I(\epsilon)\rangle = 2v_F^2 \sin\epsilon \int_R d\mathbf{Y}_1 d\mathbf{Y}_3 \int d\mathbf{R}_1 \int_T^\infty dt_1 \int_{T/2}^{t_1-T/2} dt_1' \int_T^\infty dt_3 \times \int_{T/2}^{t_3-T/2} dt_3' \langle \tilde{P}(\mathbf{Y}_1,\mathbf{R}_1;t_1-t_1')P(\mathbf{R}_1,\mathbf{Y}_{01};t_1') \times \tilde{P}(\mathbf{Y}_3,\mathbf{R}_3;t_3-t_3')P(\mathbf{R}_3,\mathbf{Y}_{03};t_3')\rangle, \quad (68)$$

where T_W is the function of ϵ given in Eq. (23). We next note that within $T_W/2$ of the crossing, paths $\gamma 1$ and $\gamma 3$ are so close to each other that their joint survival probability is given by Eq. (13). Elsewhere, $\gamma 1$ and $\gamma 3$ escape independently through either lead at any time; hence,

$$\langle I(\epsilon)\rangle = \frac{p_F^4 \tau_{D1}}{\pi\hbar m} \frac{\rho_{m_0}^2 \rho_m^2 N_m^2 \cos\theta_{01}\cos\theta_{03}\sin\epsilon}{\left(\sum_{m'} \rho_{m'} N_{m'}\right)^3} e^{-T_W(\epsilon)/\tau_{D2}}, \quad (69)$$

where we used $N_{m'}=(\pi\hbar)^{-1}p_F W_{m'}$ and assumed that the probability that $\gamma 3$ is at $\mathbf{R}_3$ at time t_3' in a system of area A is $(2\pi A)^{-1}=m[2\pi\hbar\tau_D\Sigma_{m'}\rho_{m'}N_{m'}]^{-1}$. Then, the $\mathbf{Y}_{01,03}$ integral in Eq. (67) gives $(2W_{m_0})^2$. The integral over ϵ is the same as that given in Eq. (34) for weak localization. Thus,

$$D_{2g} = -\frac{\rho_{m_0}^2 \rho_m^2 N_{m_0}^2 N_m^2 \sum_{m'} \rho_{m'}(2-\rho_{m'})N_{m'}}{\left(\sum_{m'} \rho_{m'} N_{m'}\right)^4} \exp[-\tau_E^{\mathrm{op}}/\tau_{D2}]. \quad (70)$$

Summing all the contributions in Fig. 6, given in Eqs. (65), (66), and (70), we get

$$D_2 = \frac{\rho_{m_0}^2 \rho_m^2 N_{m_0} N_m \exp[-\tau_E^{\mathrm{op}}/\tau_{D2}]}{\left(\sum_{m'} \rho_{m'} N_{m'}\right)^2} \left[N_{m_0}+N_m + \frac{2(2-\rho_{m_0}-\rho_m)N_{m_0}N_m}{\sum_{m'} \rho_{m'} N_{m'}} - \frac{N_{m_0}N_m \sum_{m'} \rho_{m'}(2-\rho_{m'})N_{m'}}{\left(\sum_{m'} \rho_{m'} N_{m'}\right)^2} \right]. \quad (71)$$

C. Total shot noise for arbitrary Ehrenfest time

Thus, we find that the Fano factor is given by

$$F = 1 - \frac{(D_1+D_2)\sum_{m'} \rho_{m'} N_{m'}}{\rho_{m_0}\rho_m N_{m_0} N_m}, \quad (72)$$

where D_1 and D_2 are given by Eqs. (63) and (71).

Let us first consider this result for transparent barriers ($\rho_{m'}=1$ for all m'); in this case, it simplifies to

$$F = \left[1 - \frac{N_{m_0}+N_m}{\sum_{m'} N_{m'}} + \frac{N_{m_0}N_m}{\left(\sum_{m'} N_{m'}\right)^2}\right] \exp[-\tau_E^{\mathrm{op}}/\tau_D], \quad (73)$$

where $\tau_D^{-1}=(\tau_0 L)^{-1}\Sigma_{m=1}^n W_m$. As noted in Refs. 8 and 17 for two leads without tunnel barriers, the contributions to $\mathrm{Tr}[\mathbb{S}_{mm_0}^\dagger \mathbb{S}_{mm_0}\mathbb{S}_{mm_0}^\dagger \mathbb{S}_{mm_0}]$ which enter or exit the cavity in a correlated manner cancel the contribution of $\mathrm{Tr}[\mathbb{S}_{mm_0}^\dagger \mathbb{S}_{mm_0}]$. In that case, the noise is given by the contribution which enters and exits the cavity in an uncorrelated manner [Fig. 6(g)]. Here, we see that this is only the case for two leads; the first term in Eq. (73) comes from $\mathrm{Tr}[\mathbb{S}_{mm_0}^\dagger \mathbb{S}_{mm_0}]$, while the second term comes from those contributions to $\mathrm{Tr}[\mathbb{S}_{mm_0}^\dagger \mathbb{S}_{mm_0}\mathbb{S}_{mm_0}^\dagger \mathbb{S}_{mm_0}]$ which enter or exit the cavity in a correlated manner; in general, these two do not cancel each other. However, we see that for an arbitrary number of leads without tunnel barriers, the paths shorter than the Ehrenfest time are noiseless (just as for two leads[17]).

Now, let us consider Eq. (72) in the limit of opaque barriers ($\rho_{m'}\to 0$ for all m'); we see from Eq. (72) that the Fano factor is

$$F = 1 - \frac{2\rho_{m_0}\rho_m N_{m_0} N_m}{\left(\sum_{m'} \rho_{m'} N_{m'}\right)^2}, \quad (74)$$

which is completely *independent* of the Ehrenfest time. In fact, when we expand Eq. (72) to $\mathcal{O}[\rho]$, we see that the $\mathcal{O}[\rho]$ term is also independent of the Ehrenfest time; thus,

$$F = 1 - \frac{2\rho_{m_0}\rho_m(1-\rho_{m_0}-\rho_m)N_{m_0}N_m}{\left(\sum_{m'} \rho_{m'} N_{m'}\right)^2} - \frac{\rho_{m_0}\rho_m N_{m_0}N_m \sum_{m'} \rho_{m'}^2 N_{m'}}{\left(\sum_{m'} \rho_{m'} N_{m'}\right)^3} - \frac{\rho_{m_0}\rho_m (N_{m_0}+N_m)}{\sum_{m'} \rho_{m'} N_{m'}} + \mathcal{O}[\rho^2], \quad (75)$$

where the $\mathcal{O}[\rho^2]$ term is dependent on the Ehrenfest time.

In the case of a symmetric two-lead cavity, $N_1=N_2=N$ and $\rho_1=\rho_2=\rho$, the rather ugly result in Eq. (72) greatly simplifies to

$$F = \frac{1-\rho}{2-\rho}(1-e^{-\tau_E^{\mathrm{op}}/\tau_{D2}}) + \frac{2-\rho}{4} e^{-\tau_E^{\mathrm{op}}/\tau_{D2}}. \quad (76)$$

Both terms in this expression increase monotonically as we reduce the transparency of the tunnel barriers from $\rho=1$ to $\rho=0$; thus, the presence of the tunnel barriers always increases the quantum noise (for given Ehrenfest time). In the limit of transparent barriers ($\rho=1$), the Fano factor crosses over from the RMT value of 1/4 to zero as we increase the Ehrenfest time, while in the limit of opaque barriers ($\rho \ll 1$), the Fano factor is 1/2, independent of the Ehrenfest time.

D. Consistency check: Alternative shot-noise formula

Finally, we note that the main difficulty in the above calculation is the identification of all contributions. Thus, it is

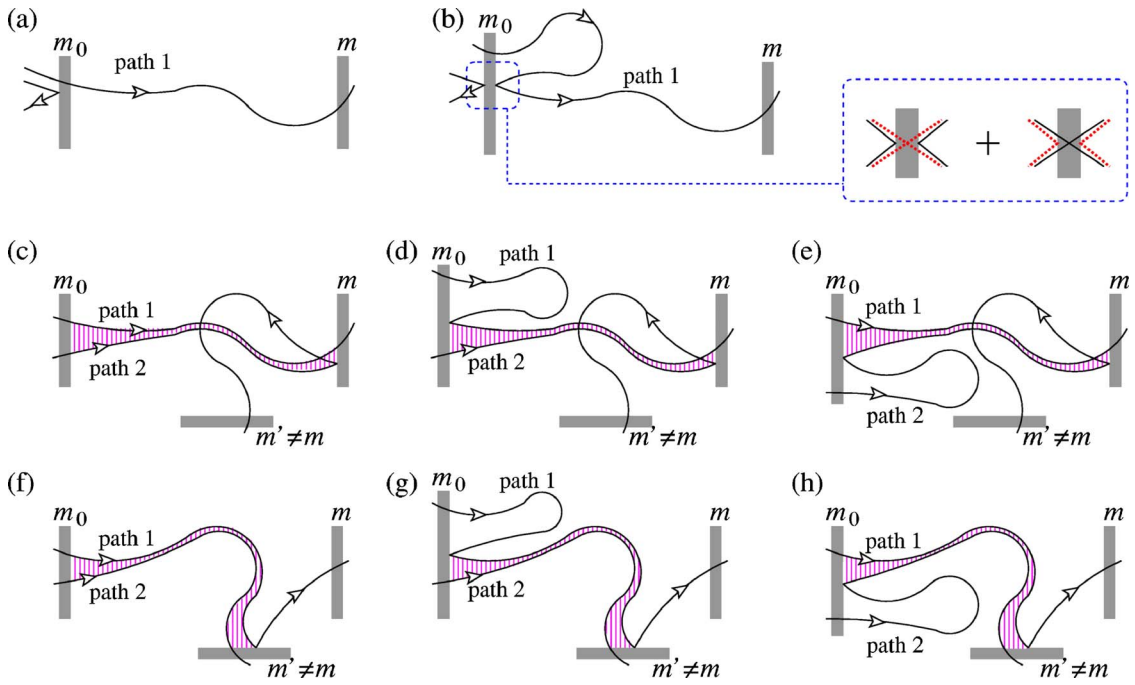

FIG. 8. (Color online) Here, we list all the contributions to $\Sigma_{m' \neq m} \mathrm{Tr}[\mathrm{S}^{\dagger}_{m'm_0} \mathrm{S}_{m'm_0} \mathrm{S}^{\dagger}_{mm_0} \mathrm{S}_{mm_0}]$ which remain finite in the limit of infinite Ehrenfest time. The contributions are drawn in the same manner as Fig. 6, with only paths 1 and 3 shown. The noise in these contribution is purely due to the stochastic nature of scattering at the tunnel barriers; if they were absent, these contributions would be noiseless. The calculation will show that (a) and (b) are independent of τ_E^{op}, while all other contributions go like $(1-e^{-\tau_E^{\mathrm{op}}/\tau_{D2}})$.

important to have an independent check that no contributions have been missed. In Appendix C, we use the fact that the Fano factor can be written in terms of a product of transmission and reflection contributions, see Eq. (C2), and rederive the result in Eq. (72) starting from that formula. The transmission and/or reflection contributions calculated there (shown in Figs. 8 and 9) combine in a nontrivial manner to give the result in Eq. (72). This can be seen by the fact that there is no obvious $m_0 \leftrightarrow m$ symmetry in the contributions in Appendix C (compare that with the contributions calculated above, where every contribution has a partner with $m_0 \leftrightarrow m$). Thus, if we miss a contribution in Figs. 6 and 7 and miss the equivalent contributions in Figs. 8 and 9, it would be extremely unlikely that the two sets of contributions would sum to give the same result.

VII. CONCLUDING REMARK

We have summarized the central physics discussed in this paper in Sec. II and recommend that as a summary of the contents of this paper. Here, we would like to reiterate one technical point which makes the semiclassical calculations tractable. It is the fact that when writing probabilities to escape into a given lead we count only successful attempts to escape (not situations where the particle hit the tunnel barrier on a lead and was reflected back into the cavity). This is very different from the equivalent RMT calculation[24] in which each collision with the tunnel barrier on a lead was explicitly taken into account, regardless of whether the particle tunnels or not. We feel unqualified to speculate if our approach could be directly applied to simplifying the RMT calculations.

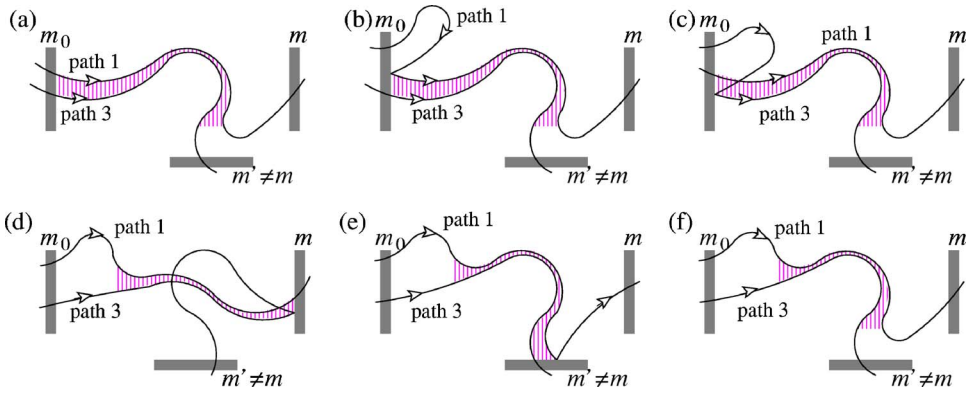

FIG. 9. (Color online) Here, we list all the contributions to $\Sigma_{m' \neq m} \mathrm{Tr}[\mathrm{S}^{\dagger}_{m'm_0} \mathrm{S}_{m'm_0} \mathrm{S}^{\dagger}_{mm_0} \mathrm{S}_{mm_0}]$ which vanish in the limit of infinite Ehrenfest time. The contributions are drawn in the same manner as Fig. 6, with only paths 1 and 3 shown. The calculation will show that all these contributions go like $e^{-\tau_E^{\mathrm{op}}/\tau_{D2}}$. Thus, for $\tau_E^{\mathrm{op}}/\tau_{D2} \to 0$, the noise is given by the sum of these contributions and (a) and (b).

However, we are certain that the hand-waving arguments made in Sec. II A would be an excellent guide to the intuition when performing involved RMT calculations.

ACKNOWLEDGMENTS

I am grateful to M. Polianski and C. Petitjean for very useful and stimulating discussions and thank Y. Nazarov for drawing my attention to this problem.

APPENDIX A: PHASE OF TRANSMISSION AND REFLECTION AT A TUNNEL BARRIER

Here, we calculate the complex transmission and reflection amplitudes, t and r, for a rectangular tunnel barrier in the limit that the barrier is thin and high (width l and height U). We follow the standard procedure explained in most quantum mechanics textbooks. We include the details here simply because most textbooks give the transmission and reflection probabilities but not the phases.

We consider a one-dimensional system with the particle coming from the left. To the left of the tunnel barrier, the solutions of Schrödinger's equation have momentum $\pm p$, while to the right of the barrier, the only nonzero solution has momentum $+p$. Inside the barrier, the solutions decay and/or grow like $\exp[\pm kx/\hbar]$, where $k=[2mU-p^2]^{1/2}$. Solving the simultaneous equations that we find by matching the wave function and its derivative at the two edges of the tunnel barrier, we see that the transmission amplitude is

$$t = \frac{\exp[-\mathrm{i}pl/\hbar]}{\cosh(kl/\hbar) + \frac{\mathrm{i}}{2}(k/p - p/k)\sinh(kl/\hbar)}, \tag{A1}$$

while the reflection amplitude is

$$r = -\frac{\mathrm{i}}{2}\frac{(k/p + p/k)\sinh(kl/\hbar)}{\cosh(kl/\hbar) + \frac{\mathrm{i}}{2}(k/p - p/k)\sinh(kl/\hbar)}, \tag{A2}$$

where l is the width of the barrier. To take the narrow and high barrier limit, we take $U\to\infty$ and $l\to 0$ such that $kl/\hbar$ remains finite. We then adjust $kl/\hbar$ to give us the tunneling probability $\rho=|t|^2$ that we wish; in this limit, $pl/\hbar=0$.

We will need the transmission and reflection phases in Appendix C, because for $\tilde{D}_{1b}$ we find that t and r do not appear in the combination $|t|^2=\rho$ or $|r|^2=1-\rho$. Instead, we need to calculate the combinations $(t^*r)^2$ and $(r^*t)^2$. From the above results for t and r, we see that

$$[(e^{\mathrm{i}pl/\hbar}t)^*r]^2 = [(e^{\mathrm{i}pl/\hbar}t)r^*]^2 = -|t|^2|r|^2 = -\rho(1-\rho), \tag{A3}$$

and hence in the thin barrier limit ($pl\ll\hbar$), we get $(t^*r)^2=(r^*t)^2=-\rho(1-\rho)$.

We note that throughout this paper, we assume that $\rho=|t|^2$ is unchanged as we take the classical limit $\lambda_F/L\to 0$. This means that we keep the ratio λ_F/l fixed (and do not scale l like the classical scales W and L) as we take the limit $\lambda_F/L\to 0$. For simplicity, we call this the *classical limit*. Now, one might argue that the strict classical limit would involve taking $\lambda_F/l\to 0$, so there would be no tunneling. However, this limit is uninteresting because without tunneling there would be no conduction at all.

APPENDIX B: APPROXIMATING SUM OVER LEAD MODES BY DIRAC δ FUNCTION

The approximation made above Eq. (19), was introduced in Refs. 17 and 18; however, the explanation given there was too brief to be helpful. The issue not discussed there was the fact that $\exp[\mathrm{i}S_\gamma/\hbar]$ in Eq. (16) oscillates as fast with y as $\langle j|y\rangle$ does. Thus, we must deal explicitly with both fast oscillating terms at once. To do this, we write path $\gamma 2$ (which goes to y') in terms of equivalent path that goes to y, and then $S_{\gamma 2}(y')=S_{\gamma 2}(y)+p_F\sin\theta'(y'-y)+\mathcal{O}[m\lambda(y'-y)^2]$. Hence, when we write $\mathrm{Tr}[\mathbb{S}^\dagger_{mm_0}\mathbb{S}_{mm_0}]$, we find that it contains $(y'-y)$ terms which oscillate fast (oscillate on a scale $\hbar/p_F=\lambda_F$); these terms are $\Sigma_n\langle y'|n\rangle\langle n|y\rangle\exp[\mathrm{i}p_F\sin\theta'(y'-y)/\hbar]$.

Evaluating the sum for an ideal lead with N lead modes of the form $\langle y|n\rangle=(2/W)^{1/2}\sin(\pi yn/W)$, one finds that

$$\sum_n \langle y'|n\rangle\langle n|y\rangle = \frac{\sin[(z'-z)(N+1/2)]}{2W\sin[(z'-z)/2]} - \frac{\sin[(z'+z)(N+1/2)]}{2W\sin[(z'+z)/2]}, \tag{B1}$$

where $z=\pi y/W$. This function is peaked at $y'=y$ with width $\sim\lambda_F$ and height $\sim\lambda_F^{-1}$, and its integral over y' is 1. Hence, $\Sigma_n\langle y'|n\rangle\langle n|y\rangle\simeq\delta(y'-y)$ for functions which vary slowly on the length scale of a Fermi wavelength, where $\delta(y')$ is a Dirac δ function. However, the crucial point for this derivation is that one can also show that $\Sigma_n\langle y'|n\rangle\times\langle n|y\rangle\exp[\mathrm{i}p_F\sin\theta'(y'-y)/\hbar]\simeq\delta(y'-y)$. To see this, we consider the integral $I=\int dy'\Sigma_n\langle y'|n\rangle\langle n|y\rangle\exp[\mathrm{i}p_F\sin\theta'(y'-y)/\hbar]$. Defining $z=\pi(y'-y)/W$, we find that

$$I \simeq (2\pi)^{-1}\int_{-\infty}^{\infty}\frac{dz}{z}[e^{\mathrm{i}[N(1+\sin\theta')+1/2]z} - e^{-\mathrm{i}[N(1-\sin\theta')+1/2]z}],$$

where we use the fact that the integral is dominated by $z\sim N^{-1}\ll 1$. The integrand is finite at $z=0$ even though the individual terms in the integrand diverge, so we can push the contour of integration infinitesimally into the lower half of the complex plane. To evaluate the integral over each term in the integrand, we note that the first (second) term converges in the upper (lower) half plane. The first term's contour is deformed into the upper-half plane but then encircles the pole at $z=0$ giving the contribution 2π. The second term's contour encircles nothing when pushed into the lower-half plane, so it contributes nothing. Thus, $I=1$, independent of the prefactors in the exponents. The integral is dominated by $z\sim N^{-1}$ (i.e., $y\sim\lambda_F$); hence,

$$\sum_n \langle y'|n\rangle\langle n|y\rangle\exp[\mathrm{i}p_F\sin\theta'(y'-y)/\hbar]\simeq\delta(y'-y),$$

for functions which vary slowly on the scale of the Fermi wavelength.

APPENDIX C: CALCULATING SHOT NOISE FROM TRANSMISSION AND/OR NONTRANSMISSION CORRELATIONS

The unitarity of the scattering matrix means that

$$\sum_{m'=1}^{n} [\mathbb{S}^\dagger]_{m'm_0}\mathbb{S}_{m'm_0} = 1. \tag{C1}$$

It follows that we can write the formula for the Fano factor in Eq. (54) as

$$F = \frac{\sum_{m'\neq m} \mathrm{Tr}[\mathbb{S}^\dagger_{m'm_0}\mathbb{S}_{m'm_0}\mathbb{S}^\dagger_{mm_0}\mathbb{S}_{mm_0}]}{\mathrm{Tr}[\mathbb{S}^\dagger_{mm_0}\mathbb{S}_{mm_0}]}. \tag{C2}$$

Thus, we see that the Fano factor is given by correlations between transmitting contributions (those going to lead m) and nontransmitting contributions (those going to any lead except m).

We now use the trajectory method to calculate this directly. We find no preservation of unitarity at the level of the individual path's contributions to Eq. (54) and individual path's contributions to Eq. (C2); it is only when we have summed all contributions to Eqs. (54) and (C2) that we find them to be equal. We use this as a check on the fact that we have included all relevant contributions and as a check on our algebra.

To calculate these contributions, we use exactly the same method as in Sec. VI. For a given contribution, one can take a contribution with the same topology in Fig. 6 and 7 and note that one of the legs goes to m' rather than m, with m' being summed over all leads except lead m. Thus, here we simply give the results for each contribution without discussing the details of the calculation. The exception to this is the contribution in Fig. 8(b) which has no analogous contribution in Sec. VI.

The first two contributions in Fig. 8 are independent of the Ehrenfest time, and they are

$$\tilde{D}_{1a} = \frac{\rho_{m_0}(1-\rho_{m_0})\rho_m N_{m_0} N_m}{\sum_{m'} \rho_{m'} N_{m'}}, \tag{C3}$$

$$\tilde{D}_{1b} = -\frac{2\rho_{m_0}^2(1-\rho_{m_0})\rho_m N_{m_0}^2 N_m}{\left(\sum_{m'} \rho_{m'} N_{m'}\right)^2}. \tag{C4}$$

Note that the negative sign in $\tilde{D}_{1b}$ is due to the tunneling and reflection phases at the tunnel barrier on the m_0th lead. Here, unlike for all other contributions, the complex tunneling amplitude t and reflection amplitude r do not appear as products of $|r|^2=\rho$ and $|t|^2=(1-\rho)$. Instead, they appear in the combination $(t^*r)^2$ or $(tr^*)^2$; thus, we need the phases of t and r. These are calculated in Appendix A, where we show that for the high, thin barriers considered in this paper, the phases generate an overall negative sign, so $(t^*r)^2=(tr^*)^2=-\rho(1-\rho)$.

All other terms in Fig. 8 go like $(1-\exp[-\tau_E^{\mathrm{op}}/\tau_{D2}])$. The sum of the next three contributions in Fig. 8 gives

$$\tilde{D}_{1(c+d+e)} = \frac{\rho_{m_0}^2\rho_m N_{m_0} N_m (1-\exp[-\tau_E^{\mathrm{op}}/\tau_{D2}])}{\left(\sum_{m'} \rho_{m'}(2-\rho_{m'})N_{m'}\right)\left(\sum_{m'} \rho_{m'} N_{m'}\right)} \times\left(\sum_{m'} \rho_{m'}(1-\rho_{m'})N_{m'} - \rho_m(1-\rho_m)N_m\right) \times\left(1+\frac{2(1-\rho_{m_0})N_{m_0}}{\sum_{m'} \rho_{m'} N_{m'}}\right). \tag{C5}$$

The sum of the final three contributions in Fig. 8 gives

$$\tilde{D}_{1(f+g+h)} = \frac{\rho_{m_0}^2\rho_m N_{m_0} N_m (1-\exp[-\tau_E^{\mathrm{op}}/\tau_{D2}])}{\left(\sum_{m'} \rho_{m'}(2-\rho_{m'})N_{m'}\right)\left(\sum_{m'} \rho_{m'} N_{m'}\right)} \times\left((1-\rho_m)\sum_{m'} \rho_{m'} N_{m'} - \rho_m(1-\rho_m)N_m\right) \times\left(1+\frac{2(1-\rho_{m_0})N_{m_0}}{\sum_{m'} \rho_{m'} N_{m'}}\right). \tag{C6}$$

The sum of all the contributions shown in Fig. 8 gives the noise in the infinite Ehrenfest time limit (when all contributions in Fig. 9 are zero) and is in agreement with the equivalent result, D_1, in Sec. VI.

We now turn to the contributions in Fig. 9. The sum of the first three contributions in Fig. 9 gives

$$\tilde{D}_{2(a+b+c)} = \frac{\rho_{m_0}^2\rho_m N_{m_0} N_m \exp[-\tau_E^{\mathrm{op}}/\tau_{D2}]}{\sum_{m'} \rho_{m'} N_{m'}}\left(1-\frac{\rho_m N_m}{\sum_{m'} \rho_{m'} N_{m'}}\right) \times\left(1+\frac{2(1-\rho_{m_0})N_{m_0}}{\sum_{m'} \rho_{m'} N_{m'}}\right). \tag{C7}$$

The other three contributions in Fig. 9 are

$$\tilde{D}_{2d} = \frac{\rho_{m_0}^2\rho_m N_{m_0}^2 N_m \exp[-\tau_E^{\mathrm{op}}/\tau_{D2}]}{\left(\sum_{m'} \rho_{m'} N_{m'}\right)^3} \times\left(\sum_{m'} \rho_{m'}(1-\rho_{m'})N_{m'} - \rho_m(1-\rho_m)N_m\right), \tag{C8}$$

$$\tilde{D}_{2e} = \frac{\rho_{m_0}^2\rho_m N_{m_0}^2 N_m \exp[-\tau_E^{\mathrm{op}}/\tau_{D2}]}{\left(\sum_{m'} \rho_{m'} N_{m'}\right)^3} \times\left((1-\rho_m)\sum_{m'} \rho_{m'} N_{m'} - \rho_m(1-\rho_m)N_m\right), \tag{C9}$$

$$\tilde{D}_{2f} = -\frac{\rho_{m_0}^2 \rho_m N_{m_0}^2 N_m \exp[-\tau_E^{op}/\tau_{D2}]}{\left(\sum_{m'} \rho_{m'} N_{m'}\right)^3} \times \left(1 - \frac{\rho_m N_m}{\sum_{m'} \rho_{m'} N_{m'}}\right) \sum_{m'} \rho_{m'}(2 - \rho_{m'}) N_{m'}. \quad \text{(C10)}$$

The sum of all the contributions shown in Fig. 9 *and* the contributions shown in Figs. 8(a) and 8(b) gives the noise in the zero Ehrenfest time limit (when all other contributions in Fig. 8 are zero) and is in agreement with the equivalent result, D_2, in Sec. VI.

Substituting the sum of all contributions in Figs. 8 and 9 into the numerator of Eq. (C2), we again arrive at the result given in Eq. (72). This shows that our method respects the unitarity of the scattering matrix (thereby conserving current) and acts as a check on the algebra.

[1] F. Haake, *Quantum Signatures of Chaos* (Springer, Berlin, 2000).
[2] K. Richter, *Semiclassical Theory of Mesoscopic Quantum Systems*, Springer Tracts in Modern Physics Vol. 161 (Springer, Berlin, 2000).
[3] M. V. Berry, Proc. R. Soc. London, Ser. A **400**, 229 (1985).
[4] M. Sieber and K. Richter, Phys. Scr., T **T90**, 128 (2001); M. Sieber, J. Phys. A **35**, L613 (2002).
[5] K. Richter and M. Sieber, Phys. Rev. Lett. **89**, 206801 (2002).
[6] S. Müller, S. Heusler, P. Braun, F. Haake, and A. Altland, Phys. Rev. Lett. **93**, 014103 (2004); Phys. Rev. E **72**, 046207 (2005) S. Heusler, S. Müller, A. Altland, P. Braun, and F. Haake, nlin.CD/0610053.
[7] S. Heusler, S. Müller, P. Braun, and F. Haake, Phys. Rev. Lett. **96**, 066804 (2006).
[8] P. Braun, S. Heusler, S. Müller, and F. Haake, J. Phys. A **39**, L159 (2006); S. Müller, S. Heusler, P. Braun, F. Haake, New J. Phys. **9**, 12 (2007).
[9] G. Berkolaiko, H. Schanz, and R. S. Whitney, Phys. Rev. Lett. **88**, 104101 (2002); J. Phys. A **36**, 8373 (2003); G. Berkolaiko, Waves Random Media **14**, S7 (2004); nlin.CD/0604025.
[10] H. Schanz, M. Puhlmann, and T. Geisel, Phys. Rev. Lett. **91**, 134101 (2003).
[11] O. Bohigas, M. J. Giannoni, and C. Schmit, Phys. Rev. Lett. **52**, 1 (1984).
[12] I. L. Aleiner and A. I. Larkin, Phys. Rev. B **54**, 14423 (1996); Phys. Rev. E **55**, R1243 (1997).
[13] O. Agam, I. Aleiner, and A. Larkin, Phys. Rev. Lett. **85**, 3153 (2000).
[14] İ. Adagideli, Phys. Rev. B **68**, 233308 (2003).
[15] R. S. Whitney and Ph. Jacquod, Phys. Rev. Lett. **94**, 116801 (2005).
[16] S. Rahav and P. W. Brouwer, Phys. Rev. Lett. **95**, 056806 (2005); Phys. Rev. B **73**, 035324 (2006).
[17] R. S. Whitney and Ph. Jacquod, Phys. Rev. Lett. **96**, 206804 (2006).
[18] Ph. Jacquod and R. S. Whitney, Phys. Rev. B **73**, 195115 (2006), see, in particular, Sec. V.
[19] S. Rahav and P. W. Brouwer, Phys. Rev. Lett. **96**, 196804 (2006).
[20] P. W. Brouwer and S. Rahav, Phys. Rev. B **74**, 075322 (2006).
[21] C. Tian, A. Altland, and P. W. Brouwer, arXiv:cond-mat/0605051 (unpublished).
[22] P. W. Brouwer and S. Rahav, arXiv:cond-mat/0606384 (unpublished).
[23] C. M. Marcus *et al.*, Chaos, Solitons Fractals **8**, 1261 (1997).
[24] P. W. Brouwer and C. W. J. Beenakker, J. Math. Phys. **37**, 4904 (1996).
[25] S. Iida, H. A. Weidenmüller, and J. A. Zuk, Phys. Rev. Lett. **64**, 583 (1990); Ann. Phys. (N.Y.) **200**, 219 (1990).
[26] M. G. Vavilov and A. I. Larkin, Phys. Rev. B **67**, 115335 (2003).
[27] For a review, see H. Schomerus and Ph. Jacquod, J. Phys. A **38**, 10663 (2005).
[28] C. Petitjean, P. Jacquod, and R. Whitney, arXiv:cond-mat/0612118 (unpublished).
[29] H. U. Baranger, R. A. Jalabert, and A. D. Stone, Phys. Rev. Lett. **70**, 3876 (1993); Chaos **3**, 665 (1993).
[30] B. R. Levy and J. B. Keller, Commun. Pure Appl. Math. **12**, 159 (1959); H. M. Nussenzveig, Ann. Phys. (N.Y.) **34**, 23 (1965); *Diffraction Effects in Semiclassical Scattering* (Cambridge University Press, Cambridge, 1992).
[31] H. U. Baranger, D. P. DiVincenzo, R. A. Jalabert, and A. D. Stone, Phys. Rev. B **44**, 10637 (1991).
[32] We neglect the lead asymmetry in the definition of $T_W(\epsilon)$. We assume $\ln[W'/W''] \sim 1$, so the assumption is good to zero order in $(\lambda \tau_{D2})^{-1}$.
[33] At this point in Ref. 18, there are typographical errors. The argument of the logarithm in T' is inverted, and the modulus signs are absent.
[34] Ya. M. Blanter and M. Büttiker, Phys. Rep. **336**, 1 (2000).